Posttranslational modifications by ADAM10 shape myeloid antigen-presenting cell homeostasis in the splenic marginal zone

Nathalie Diener[a], Jean-Fred Fontaine[b], Matthias Klein[c,d], Thomas Hieronymus[e], Florian Wanke[a], Florian C. Kurschus[a], Andreas Ludwig[f], Carl Ware[g], Paul Saftig[h], Tobias Bopp[c,d], Björn E. Clausen[a,d,1,2], and Ronald A. Backer[a,d,1,2]

[a]Institute for Molecular Medicine, Paul Klein Center for Immune Intervention, University Medical Center of the Johannes Gutenberg-University, 55131 Mainz, Germany; [b]iOME Computational Biology and Data Mining, Johannes Gutenberg-University, 55128 Mainz, Germany; [c]Institute for Immunology, Paul Klein Center for Immune Intervention, University Medical Center of the Johannes Gutenberg-University, 55131 Mainz, Germany; [d]Research Center for Immunotherapy, University Medical Center of the Johannes Gutenberg-University, 55131 Mainz, Germany; [e]Department of Cell Biology, Institute for Biomedical Engineering, Rheinisch-Westfälische Technische Hochschule Aachen, University Medical Center, 52074 Aachen, Germany; [f]Institute of Pharmacology and Toxicology, Rheinisch-Westfälische Technische Hochschule Aachen, University Medical Center, 52074 Aachen, Germany; [g]Infectious and Inflammatory Diseases Center, Sanford Burnham Prebys Medical Discovery Institute, La Jolla, CA 92037; and [h]Institute of Biochemistry, Christian-Albrechts-University Kiel, 24098 Kiel, Germany

Edited by Li Wu, Tsinghua University, Beijing, China, and accepted by Editorial Board Member Tadatsugu Taniguchi July 20, 2021 (received for review June 24, 2021)

The spleen contains phenotypically and functionally distinct conventional dendritic cell (cDC) subpopulations, termed cDC1 and cDC2, which each can be divided into several smaller and less well-characterized subsets. Despite advances in understanding the complexity of cDC ontogeny by transcriptional programming, the significance of posttranslational modifications in controlling tissue-specific cDC subset immunobiology remains elusive. Here, we identified the cell-surface–expressed A-disintegrin-and-metalloproteinase 10 (ADAM10) as an essential regulator of cDC1 and cDC2 homeostasis in the splenic marginal zone (MZ). Mice with a CD11c-specific deletion of ADAM10 ($ADAM10^{\Delta CD11c}$) exhibited a complete loss of splenic $ESAM^{hi}$ cDC2A because ADAM10 regulated the commitment, differentiation, and survival of these cells. The major pathways controlled by ADAM10 in $ESAM^{hi}$ cDC2A are Notch, signaling pathways involved in cell proliferation and survival (e.g., mTOR, PI3K/AKT, and EIF2 signaling), and EBI2-mediated localization within the MZ. In addition, we discovered that ADAM10 is a molecular switch regulating cDC2 subset heterogeneity in the spleen, as the disappearance of $ESAM^{hi}$ cDC2A in $ADAM10^{\Delta CD11c}$ mice was compensated for by the emergence of a $Clec12a^{+}$ cDC2B subset closely resembling cDC2 generally found in peripheral lymph nodes. Moreover, in $ADAM10^{\Delta CD11c}$ mice, terminal differentiation of cDC1 was abrogated, resulting in severely reduced splenic $Langerin^{+}$ cDC1 numbers. Next to the disturbed splenic cDC compartment, ADAM10 deficiency on $CD11c^{+}$ cells led to an increase in marginal metallophilic macrophage (MMM) numbers. In conclusion, our data identify ADAM10 as a molecular hub on both cDC and MMM regulating their transcriptional programming, turnover, homeostasis, and ability to shape the anatomical niche of the MZ.

A-disintegrin-and-metalloproteinase 10 | conventional dendritic cells | marginal metallophilic macrophages | Notch signaling | splenic marginal zone

The splenic marginal zone (MZ) represents a distinct and specialized structure located at the interphase between the scavenging red pulp (RP) and the lymphoid white pulp (WP). As the MZ contains the arterial gateways, it harbors highly specialized antigen-presenting cell (APC) populations that trap antigens from the circulation for their clearance and degradation, as well as the induction of adaptive immune responses. These sentinel APC include $CD11c^{+}$ conventional dendritic cells (cDC), which are scattered throughout the MZ and enriched in so-called bridging channels (1, 2), as well as $CD169^{+}$ (Siglec-1) marginal metallophilic macrophages (MMM) and $SIGN\text{-}R1^{+}$ MZ macrophages (3).

cDC are generally divided into cDC1 and cDC2 lineages (4) but can be further delineated into several distinct cDC subsets that exhibit different immune-modulatory functions (5–9). cDC1 in lymphoid organs are characterized as $CD8\alpha^{+}CD24^{+}CD205^{+}XCR1^{+}$ cells. Among cDC1, a $CD103^{+}Langerin^{+}$ subset is located predominantly in the MZ, while $Langerin^{-}$ cDC1 are situated in the WP T cell areas (10). Functionally, $Langerin^{+}$ cDC1 are primarily involved in the cross-presentation of circulating apoptotic cells, IL-12p70 production, and viral and bacterial clearance, while $Langerin^{-}$ cDC1 are less efficient in executing these tasks (1, 11–14). $CD11b^{+}SIRP\text{-}\alpha^{+}$ cDC2 on the other hand are more heterogeneous than cDC1 and express cell-surface markers that overlap with monocyte-derived DC (Mo-DC) and macrophages (15). cDC2 consist of at least two predominant lineages based on the mutually exclusive expression of the transcription factors (TF) T-bet and ROR-γt (16). $T\text{-}bet^{+}$ cDC2A

Significance

Conventional dendritic cells (cDC) and macrophages display a high phenotypic and functional heterogeneity. ADAM10 regulates diverse cellular activities via so-called ectodomain shedding of cell-surface proteins. Here, we report that mice with a CD11c-specific deletion of ADAM10 exhibit defective cDC subset homeostasis in the splenic marginal zone (MZ). Specifically, $ESAM^{hi}$ cDC2A are replaced by a $CX3CR1^{+}$ cDC2B population, and terminal differentiation of cDC1 is abrogated. Moreover, absent ADAM10 leads to the selective expansion of marginal metallophilic macrophages. Thus, ADAM10 represents an essential molecular switch on splenic antigen-presenting cells, shaping the anatomical niche of the MZ. Thereby, ADAM10-mediated posttranslational processes constitute a pathway beyond the usual and well-characterized transcriptional decisions governing tissue-specific cDC and macrophage subset commitment and homeostasis.

Author contributions: N.D., T.H., F.W., and R.A.B. performed research; N.D., J.-F.F., M.K., T.H., F.W., T.B., and R.A.B. analyzed data; F.C.K., A.L., C.W., and P.S. contributed new reagents/analytic tools; B.E.C. and R.A.B. designed research; and B.E.C. and R.A.B. wrote the paper.

The authors declare no competing interest.

This article is a PNAS Direct Submission. L.W. is a guest editor invited by the Editorial Board.

[1]B.E.C. and R.A.B. contributed equally to this work.

[2]To whom correspondence may be addressed. Email: bclausen@uni-mainz.de or r.backer@uni-mainz.de.

This article contains supporting information online at https://www.pnas.org/lookup/suppl/doi:10.1073/pnas.2111234118/-/DCSupplemental.

Published September 15, 2021.

are further characterized by CD4 and endothelial cell-selective adhesion molecule (ESAM) expression, while ROR-γt$^+$ cDC2B are ESAM^{lo} and selectively express the C-type lectin-like receptor Clec12a. ESAM^{hi} cDC2A are efficient in MHCII antigen presentation and CD4$^+$ T cell activation but poor in the production of proinflammatory cytokines, which is a characteristic of ESAM^{lo} cDC2B (17–22).

While the transcriptional programming involved in cDC1 and cDC2 subset fate commitment is partially known (7, 23–26), numerous molecular cues regulating the fine-tuning of the final differentiation and homeostasis of tissue-specific cDC subsets are still unclear (27). Proteinases of the A-disintegrin-and-metalloproteinase (ADAM) family are involved in the posttranslational modification of cell-surface proteins via a process called ectodomain shedding (28–32). Although the closely related ADAM10 and ADAM17 regulate a variety of cellular responses, such as the release of cell adhesion molecules, cytokines, and chemokines, as well as the generation of intracellular signals, for example, Notch signaling (32, 33), little is known about their role in the immune system (34). Yet, ADAM10, ADAM17, and several of their putative targets are highly expressed on myeloid cells, suggesting that these proteases are key molecules orchestrating cDC and macrophage homeostasis (28–32, 34). In line with this, ADAM10-mediated shedding of FLT3L was recently shown to be critical for the development and maintenance of splenic ESAM^{hi} cDC2A (35).

To determine the specific role of ADAM-mediated ectodomain shedding for the development and homeostasis of splenic macrophages and cDC subsets, we analyzed mice with CD11c$^+$ cell-specific genetic deficiencies of ADAM10 and/or ADAM17. Our data establish that ADAM10, but not ADAM17, represents an essential molecular switch governing critical aspects of splenic macrophage and cDC homeostasis in the MZ. Notably, ADAM10 dependence was not restricted to the ESAM^{hi} cDC2A subset but was also vital for the homeostasis of splenic XCR1$^+$Langerin$^+$ cDC1 in the MZ. Moreover, these mice exhibited differences in MMM, identifying nonredundant ADAM10-mediated posttranslational modifications as an indispensable molecular hub on CD11c$^+$ APC, fine-tuning the biology and likely also the function of the splenic MZ microenvironment.

Methods

Mice. Adam10$^{flox/flox}$ and Adam17$^{flox/flox}$ mice were generated previously (36, 37) and bred to B6.Cg-Tg(Itgax-cre)i-1Reiz/J (CD11c-Cre mice) (38) to generate Adam10$^{flox/flox}$-CD11c-Cre (ADAM10$^{\Delta CD11c}$), Adam17$^{flox/flox}$-CD11c-Cre (ADAM17$^{\Delta CD11c}$), and Adam10$^{flox/flox}$Adam17$^{flox/flox}$-CD11c-Cre (ADAM10/17$^{\Delta CD11c}$) mice, respectively. Adam10$^{flox/flox}$ mice were also crossed to CX3CR1-Cre (39) (ADAM10$^{\Delta CX3CR1}$) and XCR1-Cre (40) mice (ADAM10$^{\Delta XCR1}$). Germline transmitted EBI2$^{fl\text{-}EGFP}$ mice were crossed to the Cre deleter strain to generate EBI2-deficient EBI2$^{EGFP/EGFP}$ mice (EBI2-KO) (41). All mice were used on a C57BL/6 background and maintained under specific pathogen-free conditions at the Translational Animal Research Center of the University Medical Center Mainz (Mainz, Germany). CD11c-Cre$^+$ mice and CD11c-Cre$^-$ littermate controls were housed together to avoid cage bias, and animals (both male and female) were between 8 and 16 wk of age at the start of the experiment. All mice were used in accordance with institutional and national animal experimentation guidelines.

cDC Phenotyping by Flow Cytometry. Single cells were suspended in fluorescence-activated cell sorting (FACS) buffer (phosphate buffered saline [PBS]/2mM EDTA/2% fetal calf serum [FCS]). Immunostaining was performed in the presence of rat anti-mouse Fc-γRIII/II receptor (CD16/32; clone 2.4G2), and cells were stained with appropriate antibodies at 4 °C in the dark for 30 to 45 min. Intracellular or intranuclear staining was performed using the reagents provided in the Cytofix/Cytoperm kit according to the manufacturer's instructions (BD Biosciences). Flow cytometry was performed with a FACSCanto II or FACSymphony (both BD Biosciences), and data were analyzed using FlowJo software (TreeStar Inc). The full list of antibodies can be found in *SI Appendix*, Table S1.

Additional Methods. In vivo treatments, sample preparation and cell sorting, bone marrow-derived DC cultures, RNA sequencing, microarray data analysis, and transwell migration assays are described in *SI Appendix, Materials and Methods*.

Statistical Analysis. In all experiments, data are presented as mean ± SEM and were analyzed applying the two-tailed, unpaired Student's *t* test or one-way ANOVA with Bonferroni post hoc test, using GraphPad Prism 8 software. *P* values of <0.05 were considered statistically significant. Significance is indicated as follows: $*P < 0.05$, $**P < 0.01$, and $***P < 0.001$.

Results

ADAM10 Is Essential for the Homeostasis of Splenic Langerin$^+$ cDC1 and ESAM^{hi} cDC2. Both ADAM10 and ADAM17 are expressed on myeloid cells, including splenic cDC1 and cDC2 (Fig. 1*A*). To examine their role in regulating cDC homeostasis, we generated CD11c-specific knockouts (KO) of either ADAM (ADAM10$^{\Delta CD11c}$ and ADAM17$^{\Delta CD11c}$ mice). As conditional deletion of, respectively, ADAM10 and ADAM17 resulted in increased expression of the other ADAM on BM-DC and splenic cDC2 (*SI Appendix*, Fig. S1 *A* and *B*), we also analyzed ADAM10/17$^{\Delta CD11c}$ double-knockout (DKO) mice to exclude any possible compensatory effects.

Although splenic cDC frequencies were consistently reduced in both ADAM10$^{\Delta CD11c}$ and ADAM10/17$^{\Delta CD11c}$ mice, ADAM10 or ADAM17 deficiency did not affect absolute cDC numbers in the spleen and peripheral lymph nodes (pLN) (Fig. 1*B* and *SI Appendix*, Fig. S1 *C–E*). Moreover, the division of cDC into XCR1$^+$ cDC1 and SIRP-α$^+$ cDC2 subsets was unaffected in the spleen of ADAM10$^{\Delta CD11c}$ mice (Fig. 1*C*). ADAM10 deficiency also did not affect the cDC1/cDC2 subset distribution among resident and tissue-derived migratory cDC populations in pLN (*SI Appendix*, Fig. S1*E*). Nevertheless, unsupervised visualization of high-dimensional flow cytometry data of splenic cDC using t-distributed stochastic neighbor embedding revealed dramatic phenotypic changes within both the cDC1 and cDC2 compartment (Fig. 1*D*). In line with previous reports (35, 42), these changes could be attributed to the depletion of ESAM^{hi} cDC2 in the spleens from ADAM10$^{\Delta CD11c}$ and ADAM10/17$^{\Delta CD11c}$ but not ADAM17$^{\Delta CD11c}$ mice (Fig. 1*E* and *SI Appendix*, Fig. S1*F*). Notably, also the unique population of splenic Langerin$^+$XCR1$^+$ cDC1 was twofold reduced in ADAM10$^{\Delta CD11c}$ and ADAM10/17$^{\Delta CD11c}$ mice (Fig. 1*F* and *SI Appendix*, Fig. S1*G*). In contrast to the spleen, ADAM10 deficiency did not result in dramatic changes in the phenotype and homeostasis of cDC1 and cDC2 in pLN (*SI Appendix*, Fig. S1*H*). In line with the spleen-restricted ADAM10 dependency, nonlymphoid tissue DC populations, including Langerhans cells, dermal cDC, or pulmonary CD103$^+$ cDC1 and CD11b$^+$ cDC2, appeared similar between control and ADAM10$^{\Delta CD11c}$ mice (*SI Appendix*, Fig. S1*I*).

ADAM10 Deficiency Results in the Expansion of MMM. To examine the impact of the observed changes in the cDC1 and cDC2 compartments in the steady-state spleen, and since CD11c-Cre does not exclusively target cDC, we also analyzed other splenic cell populations in detail. Overall, there was no gross difference in the cellularity or the distribution of hematopoietic cell populations in ADAM10$^{\Delta CD11c}$ and ADAM17$^{\Delta CD11c}$ mice (*SI Appendix*, Fig. S2*A*). Plasmacytoid DC (pDC) did not differ in number in ADAM-deficient mice (*SI Appendix*, Fig. S2*B*), yet an eightfold reduction in the number of pDC-like CX$_3$CR1$^+$CD8-α$^+$XCR1$^-$ DC (43) was observed in ADAM10$^{\Delta CD11c}$ mice (*SI Appendix*, Fig. S2*C*). Moreover, eosinophils (70-fold) and monocyte-derived inflammatory DC (eightfold) were markedly increased in these mice (*SI Appendix*, Fig. S2*D*), but ADAM10 deficiency did not result in excessive immune activation, as the maturation state of cDC, determined by the expression of activation markers like CD80 and CD86, was similar to controls (*SI Appendix*, Fig. S2*E*).

Histological examination of the spleen revealed that ADAM10$^{\Delta CD11c}$ mice displayed a more diffuse and broader MZ as compared to controls (Fig. 1 *G* and *H*). Specifically, CD169$^+$ MMM were less strictly confined to the MZ but scattered across the RP and WP.

Moreover, the number of these MMM increased twofold in ADAM10$^{\Delta CD11c}$ but not ADAM17$^{\Delta CD11c}$ mice (Fig. 1*I* and *SI Appendix*, Fig. S2*F*). Of note, targeted ADAM10 deletion using CX_3CR1-Cre (expressed by mononuclear phagocytes including MMM) but not by XCR1-Cre (expressed by cDC1) resulted in a comparable twofold increase of MMM (Fig. 1*J*). Together, these data demonstrate that CD11c-specific ADAM10, but not ADAM17, uniquely contributes to the homeostasis of multiple distinct splenic APC populations in the MZ, while it is dispensable for cDC homeostasis in peripheral tissues and pLN.

Splenic Langerin$^+$ cDC1 Selectively Depend on ADAM10. cDC1 in the spleen consist of CD103$^+$ and CD103$^-$ subpopulations (11), where about half of the CD103$^+$ cells coexpress Langerin. The frequency of these Langerin$^+$CD103$^+$ cDC1 was strongly diminished in the spleens of ADAM10$^{\Delta CD11c}$ mice (Fig. 2*A*). Intriguingly, splenic cDC1 total counts were maintained due to the expansion of Langerin-negative cDC1 (Fig. 2*B*). Although ESAM is predominantly expressed on cDC2 (17, 44), ESAM$^+$ cells were enriched within the Langerin-expressing cDC1 fraction, and an approximately twofold reduction of this cDC1 subset was observed in ADAM10$^{\Delta CD11c}$ mice (Fig. 2*C*). Since Langerin$^+$XCR1$^+$ cDC1

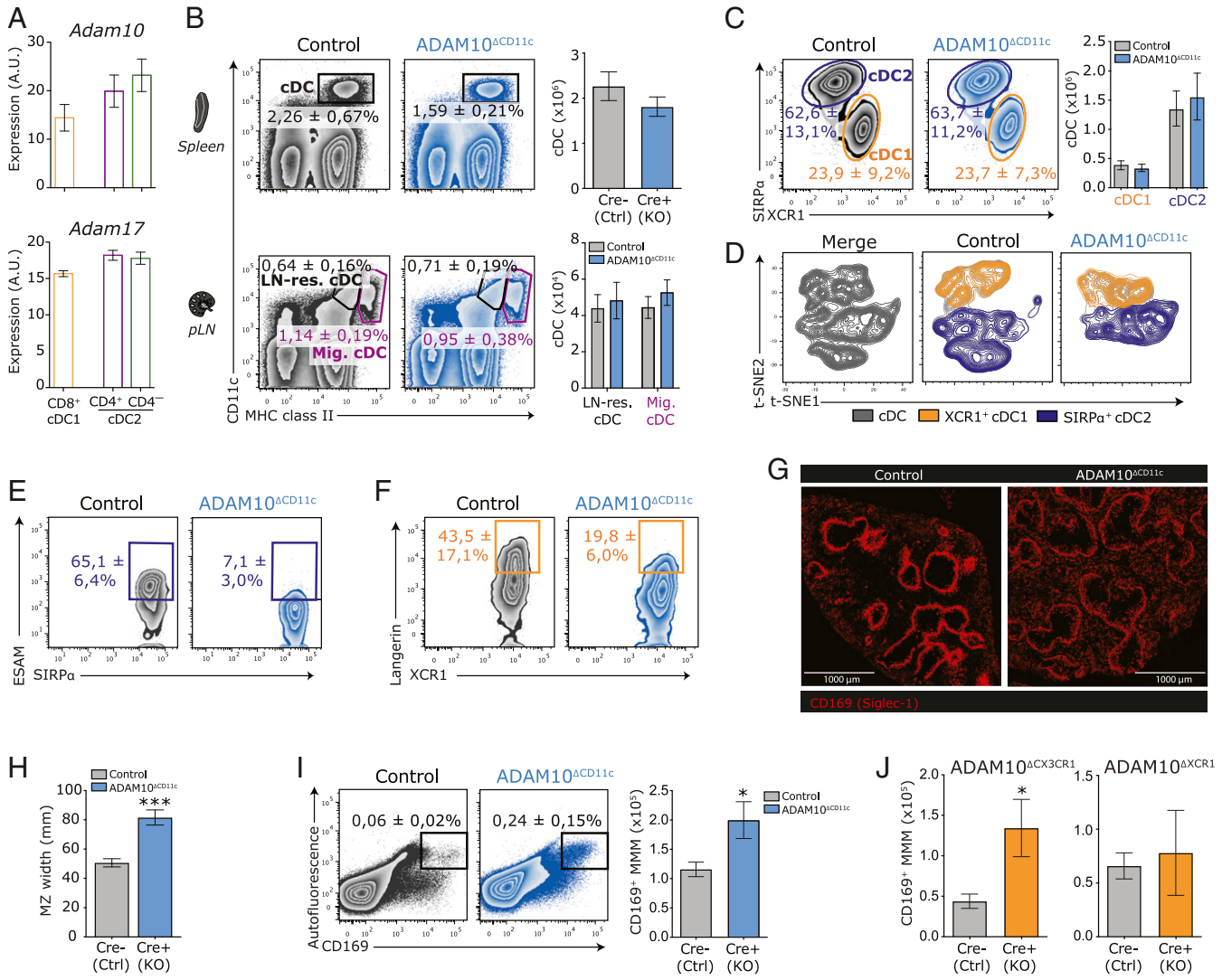

Fig. 1. ADAM10-mediated modifications are essential for the homeostasis of splenic ESAM^{hi} cDC2 and Langerin$^+$ cDC1. (*A*) Abundance of mRNA encoding ADAM10 (*Top*) or ADAM17 (*Bottom*) in bulk-sorted splenic CD11c$^+$MHCII$^+$ CD8-α$^+$ cDC1 (orange), CD4$^+$ cDC2 (purple), and CD4$^-$ cDC2 (green) subsets presented in arbitrary units (AU). (*B*) Frequencies (flow cytometry plots) and absolute numbers (bar graphs) of splenic CD11c$^+$MHCII$^+$ cDC (*Top*) and CD11c^{hi}MHCII$^+$ LN-resident cDC and CD11c$^+$MHCII^{hi} LN-migratory cDC (*Bottom*) in control versus ADAM10$^{\Delta CD11c}$ mice. (*C*) Representative flow cytometry plots showing frequencies of splenic XCR1$^+$ cDC1 (orange gate) and SIRP-α$^+$ cDC2 (aubergine gate) within the CD11c$^+$MHCII$^+$ cDC gate of control and ADAM10$^{\Delta CD11c}$ mice. Bar graphs indicate absolute numbers of XCR1$^+$ cDC1 and SIRP-α$^+$ cDC2 in spleens of control and ADAM10$^{\Delta CD11c}$ mice. (*D*) t-distributed stochastic neighbor embedding (t-SNE) embedding of three control and three ADAM10-KO concatenated samples with 4.000 cDC each, indicating cDC1 (orange) and cDC2 (aubergine) classification based on XCR1 and SIRP-α expression, respectively. (*E*) Representative flow cytometry plot with average frequencies of splenic ESAM^{hi}SIRP-α$^+$ cDC2 in control and ADAM10$^{\Delta CD11c}$ mice. (*F*) Representative flow cytometry plot with average frequencies of splenic Langerin$^+$XCR1$^+$ cDC1 in control and ADAM10$^{\Delta CD11c}$ mice. (*G*) Immunofluorescence staining of anti-CD169 (Siglec-1) in spleens of control and ADAM10$^{\Delta CD11c}$ mice (Olympus IX81, 10×). (*H*) Bar graph represents MZ width, as determined by measuring the size of the MMM ring at four opposite locations of at least 10 MZ of three to four animals per group with Olympus CellSense Dimension software. (*I*) Frequency (representative FACS plots) and quantification (bar graphs) of total MMM numbers in spleen of control and ADAM10$^{\Delta CD11c}$ mice. MMM were characterized as living CD45$^+$ autofluorescent CD169$^+$ cells. (*J*) Quantification of MMM numbers in spleen of control, ADAM10$^{\Delta CX3CR1}$ (*Left*), and ADAM10$^{\Delta XCR1}$ (*Right*) mice. *P < 0.05 and ***P < 0.001 (Student's t test). FACS plots show one representative mouse/group with mean frequencies or mean fluorescent intensities ± SEM. Data are pooled from at least three experiments (n = 4 to 6 mice/experiment).

are considered to represent a final cDC1 maturation stage (1), we further phenotypically characterized the XCR1$^+$ cDC1 population in control and ADAM10$^{\Delta CD11c}$ mice. Indeed, the fraction of CD8-α–negative cells among XCR1$^+$ cDC1 was substantially increased in ADAM10$^{\Delta CD11c}$ mice, and ADAM10-deficient cDC1 exhibited increased CD24 expression suggesting a less differentiated state of these cells (Fig. 2*D*).

XCR1$^+$ cDC1 are distributed between the WP T cell area and the RP (45–48), while the Langerin$^+$ subset specifically resides in the MZ (1). In vivo labeling of cDC revealed that, in contrast to control cDC1, ADAM10-deficient XCR1$^+$ cDC1 preferentially localized to sites in the spleen that are accessible to intravenously injected anti-CD11c antibodies, that is, in the RP (Fig. 2*E*). To study whether ADAM10 directly controls the terminal differentiation of Langerin$^+$ cDC1, or whether the loss of these cells is secondary to the defect in MZ microarchitecture, we analyzed this cDC1 subset in ADAM10$^{\Delta XCR1}$ and ADAM10$^{\Delta CX3CR1}$ mice and found that the number of Langerin$^+$ cDC1 was significantly decreased in the spleens of both mice (Fig. 2*F*). As the splenic MZ architecture in ADAM10$^{\Delta XCR1}$ mice was unaffected, these data indicate that ADAM10 is intrinsically required for the commitment and homeostasis of Langerin$^+$ cDC1. On the other hand, the number of Langerin$^+$ cDC1 was also strongly diminished in ADAM10$^{\Delta CX3CR1}$ mice, which might suggest that indirect effects of absent ADAM10 shedding on macrophages shape appropriate cDC1 homeostasis (Fig. 2*F*).

To identify ADAM10-regulated pathways in cDC1, we performed single-cell RNA sequencing (SC-seq-WTA) of splenic CD11c$^+$ cells from control and ADAM10$^{\Delta CD11c}$ mice. This analysis revealed extensive transcriptional changes in ADAM10-deficient XCR1$^+$ cDC1 with a down-regulation of numerous genes that characterize Langerin$^+$CD103$^+$ cDC1 (11), including *Cd207* (encoding for Langerin) and *Itgae* (encoding for CD103) upon loss of ADAM10 in cDC1 (Fig. 2*G* and Dataset S1). The expression of cDC1-defining TF was not affected in ADAM10-deficient cDC1, although *Irf8* and *Id2* were slightly increased (*SI Appendix*, Fig. S3*A*). GO enrichment analysis identified that mainly biological processes involved in cDC function rather than development were affected by ADAM10 deficiency (*SI Appendix*, Fig. S3*B*), indicating that ADAM10 is dispensable for cDC1 commitment but required for their terminal differentiation into Langerin$^+$ cDC1. Collectively, these data point toward foiled terminal differentiation of splenic XCR1$^+$ cDC1 in the absence of ADAM10 on CD11c$^+$ cells.

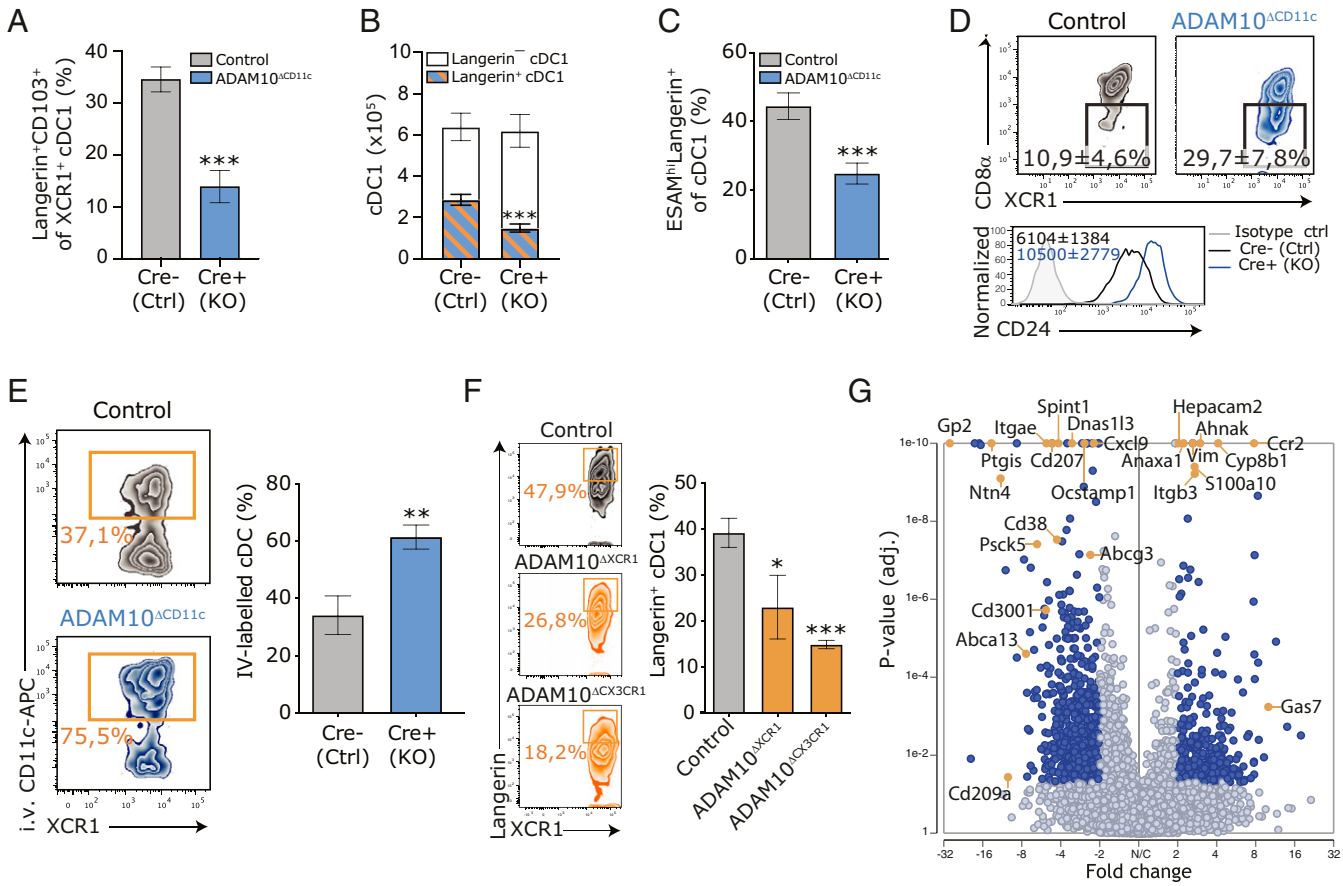

Fig. 2. ADAM10 controls the terminal differentiation of splenic Langerin$^+$ cDC1. (*A*) Frequency of Langerin$^+$CD103$^+$ cells within the XCR1$^+$ cDC1 cDC population in spleens of control and ADAM10$^{\Delta CD11c}$ mice. (*B*) Absolute numbers of splenic Langerin$^+$ and Langerin$^-$ cDC1 in control and ADAM10$^{\Delta CD11c}$ mice. (*C*) Frequency of ESAM^{hi} cells within the Langerin$^+$ cDC1 subset. (*D*) Expression of CD8-α and CD24 on splenic cDC1 isolated from control and ADAM10$^{\Delta CD11c}$ mice, assessed by flow cytometry gated on CD11c$^+$MHCII$^+$XCR1$^+$ cells. Filled histogram: isotype control. (*E*) Frequency of in vivo CD11c-labeled cDC1 in spleens of control and ADAM10$^{\Delta CD11c}$ mice. (*F*) Representative flow cytometry plot showing the frequency of splenic Langerin$^+$XCR1$^+$ cDC1 in control (*Top*), ADAM10$^{\Delta XCR1}$ (*Middle*), and ADAM10$^{\Delta CX3CR1}$ (*Bottom*) mice. Bar graph indicates the average frequency of these cells found in the spleen of the indicated mice. (G) Volcano plot representing the gene expression changes in splenic cDC1 from ADAM10$^{\Delta CD11c}$/control mice (*P* value versus $\log_2$ fold change). Genes also significantly changed in CD103$^+$ versus CD103$^-$ cDC1 are indicated in red (published dataset) (11). $^*P < 0.05$, $^{**}P < 0.01$, and $^{***}P < 0.001$ (Student's *t* test or one-way ANOVA). FACS plots show one representative mouse/group with mean frequencies or mean fluorescent intensities ± SEM. Data are pooled from at least three experiments (n = 4 to 6 mice/experiment). SC-seq-WTA is a visualization of three Cre-negative and three Cre-positive ADAM10$^{\Delta CD11c}$ mice.

Loss of Splenic ESAM^{hi} cDC2 in ADAM10$^{\Delta CD11c}$ Mice Is Compensated for by Emerging Clec12a^{+}CX$_3$CR1^{+}ESAM^{lo} cDC2B. Spleens of ADAM10$^{\Delta CD11c}$ mice were almost completely depleted of ESAM^{hi} cDC2 (Fig. 1*E*) (35, 42). However, ADAM10 deficiency did not affect total SIRP-α^{+} cDC2 counts in the spleen, as ESAM^{lo} cells strongly expanded in these mice, thereby maintaining the physiologic levels of total splenic cDC2 (Fig. 3*A*). The classical delineation of SIRP-α^{+} cDC2 into CD4^{+} and CD4^{-} subpopulations indicated that these expanding ESAM^{lo} cells could be further characterized by low CD4 but high CX$_3$CR1 and CD11b expression (Fig. 3*B*). Although ESAM^{hi} cDC2A were present in normal number in ADAM10$^{\Delta XCR1}$ mice, these cells were significantly decreased in ADAM10$^{\Delta CX3CR1}$ mice (Fig. 3*C*). ADAM10-deficient cDC2 showed normal expression of cDC2-defining TF, although *Relb*, *Stat3*, and *Ikaros* (*Ikzf1*) were significantly decreased (*SI Appendix*, Fig. S4*A*). RUNX3 cooperates with ZBTB46 to control ESAM^{hi} cDC2 homeostasis, as lack of RUNX3 shifts gene expression toward ESAM^{lo} cells and leads to a loss of the ESAM^{hi} identity (49). Accordingly, ADAM10-deficient cDC2 showed a trend toward reduced expression of both *Runx3* and *Zbtb46* transcripts, while *Zeb2* was increased (*SI Appendix*, Fig. S4*A*).

Notably, differential clustering of SC-seq-WTA data revealed that the increase in splenic ESAM^{lo}SIRP-α^{+} cDC2 in ADAM10$^{\Delta CD11c}$ mice was not due to a simple expansion of the small ESAM^{lo} cDC2 population already present in the steady-state spleen (Fig. 3*D*, subpopulation II) but that ADAM10 deficiency resulted in the emergence of a unique splenic cDC2 subpopulation (Fig. 3*D*, subpopulation III) that was transcriptionally different from splenic CD4^{-} (ESAM^{lo}) cDC2 in control mice.

ESAM^{lo} cDC2 in the spleen of ADAM10$^{\Delta CD11c}$ mice have been suggested to originate from circulating monocytes, as these cells display a myeloid signature (35). Indeed, ADAM10-deficient ESAM^{lo} cDC2 appear like Mo-DC, as they expressed high levels of Ly6C (Fig. 3*E*). Moreover, analysis of the top 15 most significant gene expression features between the cDC2 subpopulations revealed that the emerging ESAM^{lo} cDC2 (population III) displayed higher transcript levels of markers, which are typical of the monocyte/macrophage lineage, including lysozyme 1 and 2, and the mannose receptor 1 (CD206) (*SI Appendix*, Fig. S4*B*). On the other hand, splenic ESAM^{lo} cDC2 in ADAM10$^{\Delta CD11c}$ mice express FLT3 (Fig. 3*F*), a receptor that is selectively expressed on pre-DC–derived DC but not on Mo-DC (50). Moreover, emerging ESAM^{lo} cDC2 could not be characterized as genuine CD11b^{+}Ly6C^{+}CD64^{+} Mo-DC (*SI Appendix*, Fig. S4*C*) (51) or CD26^{+}CD64^{+}MAR-1^{+} inflammatory cDC2 (*SI Appendix*, Fig. S4*D*) (52).

Recently, SIRP-α^{+} cDC2 were divided into ESAM^{hi} cDC2A and Clec12a^{+} cDC2B lineages (16). Indeed, the expanding ESAM^{lo} cDC2 expressed Clec12a (Fig. 3*G*). Moreover, ADAM10-deficient cDC2 exhibited higher expression of ROR-γt, both on messenger RNA (mRNA) and protein level, while T-bet was significantly reduced as compared to control cDC2 (Fig. 3 *H* and *I*). Within ADAM10-deficient cDC2, the expression of cDC2A signature genes was markedly decreased (down-regulation of 44 out of 69 cDC2A core genes), whereas cDC2B signature genes were enriched in these cells (up-regulation of 133 out of 155 cDC2B core genes) (16) (Fig. 3*J* and Dataset S2). In addition, the cDC2A signature gene set (16) significantly overlapped with our SC-seq-WTA population I, whereas cDC2B signature genes were enriched in population III (Fig. 3*J*), indicating that the emerging ESAM^{lo} cDC2 comprise a bona fide cDC2B population.

Interestingly, steady-state pLN-resident cDC2 appeared ESAM^{lo} and expressed various Mo-DC markers, including Ly6C and Clec12a, at higher levels and frequency than their splenic counterparts, thereby phenocopying the emerging splenic ESAM^{lo} cDC2B subset in ADAM10$^{\Delta CD11c}$ mice (Fig. 3*E*). To delineate the relationship between cDC2 subpopulations in the spleen and pLN, molecular definitions of cDC subsets in these organs were generated using published gene expression data of wild-type (WT) splenic CD4^{+} cDC2 and WT pLN-derived CD4^{+} cDC2 (53) and compared to the NGS expression profiles of splenic ADAM10-deficient cDC2. This revealed that the expression of selected Mo-DC–associated genes was elevated in both ADAM10-deficient CD4^{+} and CD4^{-} cDC2 and that these specific genes were also highly expressed in WT pLN-resident cDC2 (*SI Appendix*, Fig. S4 *E* and *F* and Dataset S3). Vice versa, certain splenic cDC2-associated factors specifically decreased in WT pLN-resident cDC2 were also down-regulated in splenic ADAM10-deficient cDC2B (*SI Appendix*, Fig. S4 *E* and *F* and Dataset S3). Significantly, overlay of the WT spleen/pLN identities with our ADAM10$^{\Delta CD11c}$ SC-seq-WTA data confirmed that the WT splenic cDC2 identity overlapped with the splenic cDC2A (subpopulation I), while the pLN-associated gene signature was specifically enriched in the emerging cDC2B found in ADAM10$^{\Delta CD11c}$ mice (subpopulation III) (Fig. 3*K*). Moreover, principal component analysis of NGS data analysis of splenic ADAM10-deficient, ADAM10-control cDC2 subsets, and WT spleen/pLN cDC resulted in the clustering of splenic WT CD4^{+} cDC2 with CD4^{+}, as well as CD4^{-} cDC2 isolated from ADAM10-control animals, while both ADAM10-deficient splenic CD4^{+} and CD4^{-} cDC2 subsets rather grouped with WT CD4^{+} pLN-derived cDC2 (*SI Appendix*, Fig. S4*G*), showing that loss of ADAM10 altered gene expression of the residual cDC2A to a profile similar to the emerging ESAMlo cDC2B in ADAM10$^{\Delta CD11c}$ mice. In conclusion, rather than a monocyte association, our data strongly point out that the emerging splenic cDC2B in ADAM10$^{\Delta CD11c}$ mice represent a bona fide cDC2 subset closely related to pLN-resident cDC2 and highlight further heterogeneity within the cDC2B population.

ADAM10 Governs the Commitment, Development, and Survival of Splenic cDC2. To unravel how ADAM10 deficiency regulates the homeostasis of spleen-specific cDC subsets, we investigated the development of cDC and their precursors in ADAM10$^{\Delta CD11c}$ mice. As CD11c-cre–mediated deletion of ADAM10 occurs only downstream of the common DC precursor (CDP) stage (54, 55), we did not observe any differences in the number of common monocyte-DC precursors and CDP in the BM between ADAM10$^{\Delta CD11c}$ and control mice (*SI Appendix*, Fig. S5*A*). Also, the committed cDC precursor (pre-DC) compartment in the blood and spleen was unperturbed in ADAM10$^{\Delta CD11c}$ mice (*SI Appendix*, Fig. S5*B*). Besides, in vitro DC differentiation from BM progenitors in the presence of recombinant FLT3L did not result in different cell yields of CD24^{+} cDC1 and CD11b^{+} cDC2 equivalents (*SI Appendix*, Fig. S5*C*), demonstrating that ADAM10 is not essential for early cDC development. Based on high or low Ly6C expression, pre-DC in the spleen can be divided into precursors precommitted to either the cDC2 or cDC1 lineage (54, 56, 57). Although ADAM10$^{\Delta CD11c}$ mice exhibited increased numbers of committed CD11c^{lo}Ly6C^{+} pre-DC2 in the spleen (Fig. 4*A*), ADAM10 deficiency did impair further differentiation into CD11c^{hi}SIRP-α^{+} pre-DC2 and instead diverted progenitors toward CD24^{+} pre-DC1 development (17, 54) (Fig. 4*B*). This indicates that ADAM10-deficient committed splenic pre-DC are unable to support substantial cDC2 development in vivo.

Side-by-side analysis of enriched pathways using GO terms and Canonical Pathway Analysis (IPA) from RNA sequencing data of flow cytometry sorted CD4^{+} (ESAM^{hi}) and CD4^{-} (ESAM^{lo}) cDC2 cells revealed that in ADAM10-deficient cDC2A pathways associated with cell cycle, energy metabolism, and migration were significantly enriched for down-regulated genes, while many key pathways associated with cellular processes, cell signaling, and development were enriched for up-regulated genes (*SI Appendix*, Fig. S5*D*). Considering these changes in canonical pathways associated with energy metabolism and cell proliferation, we sought to determine whether ADAM10 deficiency negatively affected ESAM^{hi} cDC2A turnover and survival. For this, proliferation (in vivo incorporation of BrdU) and apoptosis (Annexin V/7AAD binding) of control and ADAM10-deficient splenic cDC was

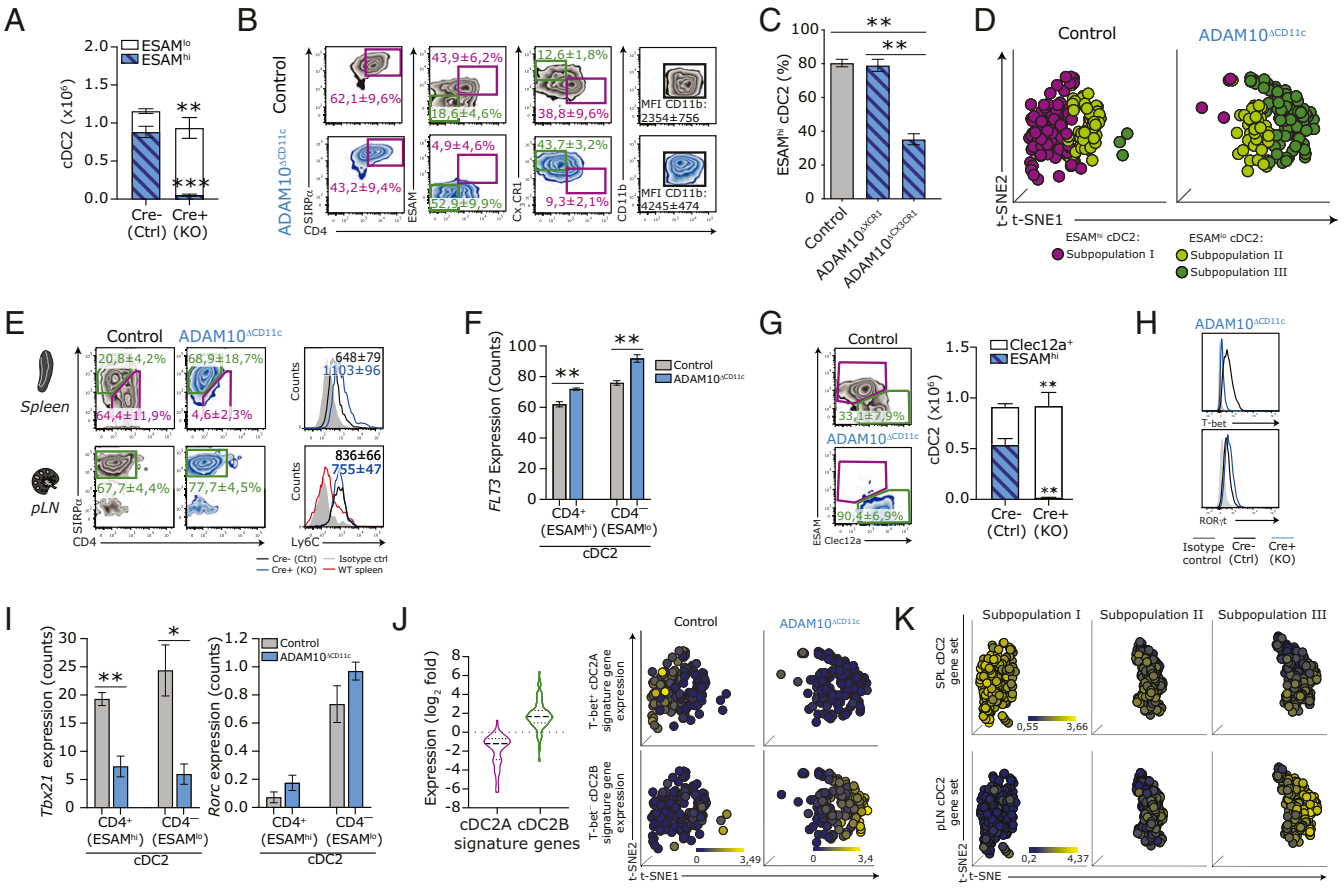

Fig. 3. ADAM10 deficiency results in the selective absence of splenic ESAM^{hi} cDC2A that is compensated for by an emerging Clec12a^{+} cDC2B subset. (*A*) Absolute cell counts of splenic ESAM^{hi} and ESAM^{lo} SIRP-α^{+} cDC2 in control and ADAM10$^{\Delta CD11c}$ mice. (*B*) Phenotypic comparison of splenic CD11c^{+}MHCII^{+}SIRP-α^{+} cDC2 isolated from control (*Top*) and ADAM10$^{\Delta CD11c}$ (*Bottom*) mice, assessed by flow cytometry. (*C*) Frequency of splenic ESAM^{hi} cDC2 in control, ADAM10$^{\Delta XCR1}$, and ADAM10$^{\Delta CX3CR1}$ mice. (*D*) t-distributed stochastic neighbor embedding (t-SNE) analysis of SC-seq-WTA profiled control and ADAM10-deficient cDC2 (gated for cells expressing *Itgax*, *H2ab1*, and *Sirpa*) showing automated clustering into an ESAM^{hi} cDC2 subpopulation (subpopulation I, purple) and two ESAM^{lo} cDC2 subpopulations (subpopulations II and III, green). Each dot represents an individual cell. (*E*) Comparison of the expression of CX_3CR1 versus ESAM and Ly6C on SIRP-α^{+} cDC2 in spleen (*Top*) and pLN (*Bottom*) from control and ADAM10$^{\Delta CD11c}$ mice assessed by flow cytometry. Filled gray histogram: isotype control. (*F*) *Flt3* RNA expression (Reads Per Kilobase Million) in splenic CD4^{+} and CD4^{-} cDC2 subsets from control and ADAM10$^{\Delta CD11c}$ mice. (*G*) Flow cytometry plots show the frequency of Clec12a^{+}SIRP-α^{+} splenic cDC2 in control and ADAM10$^{\Delta CD11c}$ mice, while bar graphs represent the absolute numbers of ESAM^{hi} and Clec12a^{+} cDC2. T-bet and Ror-γT expression, either as protein expression on control and ADAM10-deficient SIRP-α^{+} cDC2 determined by flow cytometry (*H*) or as RNA counts (Reads Per Kilobase Million) in bulk-sorted splenic CD11c^{+}MHCII^{+}CD4^{+} cDC2 (*I*). (*J*, *Left*) Violin plots show the expression of 69 Tbet^{+} cDC2A-associated key signature genes (purple) and 155 Tbet^{-} cDC2B-associated key signature genes (green) across bulk-sorted CD4^{+} cDC2 subsets. Expression is $\log_2$ fold change between ADAM10 deficient/control. Gene sets are retrieved from published database and accessible as GEO GSE130201 (16). (*Right*) Unbiased t-SNE representation of SC-seq-WTA depicting cDC2 subpopulations I through III (*Left*, as in C), indicating the expression levels of the cDC2A-associated gene signature (*Top*) and the cDC2B-associated gene signature (*Bottom*) in these cDC2 subpopulations. Each dot represents an individual cell. (*K*) Unbiased t-SNE representation of SC-seq-WTA depicting cDC2 subpopulations I through III (*Left*, as in C), indicating the expression levels of splenic cDC2-associated gene signature (comprised of 464 genes, *Top*) and the pLN-resident cDC2-associated gene signature (comprised of 184 genes, *Bottom*) in the indicated cDC2 subpopulations. Each dot represents an individual cell. *$P < 0.05$, **$P < 0.01$, and ***$P < 0.001$ (Student's *t* test), FACS plots show one representative mouse/group. Data are mean frequencies or mean fluorescent intensities ± SEM of more than five pooled experiments (n = 3 to 5 mice/experiment). RNA expression data are from three Cre-negative and three Cre-positive ADAM10$^{\Delta CD11c}$ mice.

assessed. Although the homeostatic proliferation of pre-DC in BM and spleen (54, 55, 58, 59) was not impaired (*SI Appendix*, Fig. S5*E*), BrdU labeling of splenic SIRP-α^{+} pre-cDC2 was significantly reduced in ADAM10$^{\Delta CD11c}$ mice as compared to controls (Fig. 4*C*). Also, among differentiated ESAM^{hi} cDC2, the frequency of BrdU^{+} cells upon pulse labeling was diminished (Fig. 4*D*). Surprisingly, the frequency of the cell-proliferation antigen Ki-67^{+} cells among the few remaining ADAM10-deficient ESAM^{hi} cDC2A was increased (Fig. 4*E*), suggesting that these cells prepared for cell-cycle entry but failed to progress with cell division. Consistently, the gene expression signature for G1/S and G2/M cell-cycle phases (60) was markedly decreased in ADAM10-deficient cDC2 but not in ADAM10-deficient cDC1 as compared to controls (Fig. 4*F* and Dataset S4). The few remaining ESAM^{hi} cDC2A isolated from ADAM10-deficient mice displayed an increased frequency of apoptotic cells, while the ESAM^{lo} cDC2B and cDC1 populations were not affected (Fig. 4*G*). Expression of IRF4, essential for final cDC2 differentiation and survival (61–65), was diminished in ADAM10-deficient cDC2 as compared to controls (Fig. 4*H*). Although the expression of the death receptor FAS was increased on ADAM10-deficient cDC2 (Fig. 4*I*), we did not detect any differences in active caspase 3 levels between cDC isolated from ADAM10$^{\Delta CD11c}$ and control mice, suggesting that caspase-independent pathways are involved. Collectively, these data highlight that ADAM10 critically regulates the proliferation, differentiation, survival, and metabolic state of splenic cDC2A.

ADAM10 Controls Both Notch2-Dependent and Notch2-Independent Pathways in Splenic cDC2. ADAM10 has recently been implicated to be essential for maintaining in vivo cDC2 homeostasis by shedding autocrine FLT3L from cDC2 (35). We could confirm that ADAM10-deficient cDC2 exhibited higher FLT3 expression than control cDC2 (Fig. 5*A*), possibly in response to FLT3L deprivation in situ. In agreement, signaling pathways downstream of FLT3 such as mTOR, PI3K/AKT, ERK, and FOXO3 were down-regulated in ADAM10-deficient cDC2A (Fig. 5*B*). Treatment of ADAM10$^{\Delta CD11c}$ mice with recombinant FLT3L (rFLT3L) resulted in a more robust expansion of cDC as compared to control mice (Fig. 5*C*). Although both Langerin$^+$ and Langerin$^-$ cDC1 expanded in control mice, rFLT3L supplementation could not restore splenic Langerin$^+$ cDC1 numbers in ADAM10$^{\Delta CD11c}$ mice, despite the fact that the expansion of these cells on a cell-based level was stronger than found in control mice (2.6-fold increase of Langerin$^+$ cDC1 in control mice as comparted to a 7.9-fold increase in ADAM10$^{\Delta CD11c}$ mice upon rFLT3L treatment) (Fig. 5*D* and *SI Appendix*, Fig. S6*A*). In contrast to the findings of an earlier study (35), rFLT3L treatment did not affect the number of splenic ESAM^{hi} cDC2A in both control and ADAM10$^{\Delta CD11c}$ mice, and as a consequence, rFLT3L did not restore the ESAM^{hi} phenotype in the ADAM10-deficient setting but rather resulted in a strong expansion of CX$_3$CR1$^+$ cDC2B, supporting their conventional DC origin (Fig. 5*E* and *SI Appendix*, Fig. S6*B*). These data suggest that although ADAM10 is essential for autocrine FLT3L shedding (35), this pathway does not contribute to the development and maintenance of splenic Langerin$^+$ cDC1 and ESAM^{hi} cDC2A in ADAM10$^{\Delta CD11c}$ mice.

Next to cell-intrinsic control by certain TF, Notch2 and lymphotoxin (LT-α1β2)-LT-βR signaling locally control the tissue-specific development and/or homeostasis or proliferation of ESAM^{hi} cDC2 (17, 38, 44, 58, 66). As ADAMs have been implicated in the shedding of both LT-α1β2 (67) and Notch2 (68), our data suggest that the drop in ESAM^{hi} cDC2A may be due to impaired LT-βR and/or Notch2 signaling. Although ADAM10 deficiency resulted in a small but significant increase in *Ltbr* gene expression (Fig. 5*F*), this did not translate into changes at the protein level. In contrast, ADAM10-deficient cDC2A exhibited significantly reduced levels of mRNA encoding for the NF-κB–inducing kinase (NIK) and RelB, which are both components of the downstream LT-βR signaling pathway (Fig. 5*F*). To test whether activation of LT-βR signaling could rescue the cDC2 phenotype observed in ADAM10$^{\Delta CD11c}$ mice, the animals were treated for 6 d with agonistic LT-βR antibodies (66, 69). Although anti–LT-βR treatment reduced the frequency of apoptotic cDC2 in ADAM10-sufficient animals, it failed to restore the ESAM^{hi} cDC2A and Langerin$^+$ cDC1 in ADAM10$^{\Delta CD11c}$ mice (Fig. 5*G*) nor did it lower the expression of CD11b and CX$_3$CR1 on cDC2.

Notch2 facilitates terminal differentiation and homeostasis of tissue-specific cDC, in particular of the ESAM^{hi} cDC2A subset in the spleen (17, 38, 44). Flow cytometry analysis revealed a significant up-regulation of the Notch2 receptor on ADAM10-deficient cDC2 (Fig. 5*H*), suggesting impaired ligand-mediated down modulation in the absence of ADAM10 shedding.

To address whether ADAM10 functions as a fate switch regulating splenic ESAM^{hi} cDC2 homeostasis via Notch2 (17, 44), we compared NGS data of control versus ADAM10-deficient cDC2 subsets with reanalyzed published gene expression microarray data of Notch2-KO CD11b$^+$ cDC2 (Dataset S5*A*) (44). This comparison revealed that the gene expression signature of ADAM10-deficient CD4$^+$ cDC2A highly correlated with Notch2-KO cDC2, as the expression of 437 out of 530 identified Notch2-dependent genes (82%) was also significantly changed in ADAM10-deficient cells. Additionally, also CD4$^-$ cDC2B displayed a significant overlap with Notch2-KO cells (288 out of 530 Notch2-dependent genes were changed) (Fig. 5*I* and Dataset S5*B*), including down-regulation of the well-characterized canonical Notch2-target genes *Dtx1*, *Hes1*, and *Hey1* (*SI Appendix*, Fig. S6*C*). These observations strongly suggest that in the absence of ADAM10 shedding, splenic cDC2 fail to induce Notch2-mediated terminal differentiation into ESAM^{hi} cDC2A. Intriguingly, next to the Notch2 signature in ADAM10-deficient cDC2, an even larger number of Notch2-independent genes (1,002 out of 1,439 genes in CD4$^+$ cDC2A [70%], and 620 out of 919 genes in CD4$^-$ cDC2B [67%]) differed significantly between control and ADAM10-deficient cDC2, indicating that ADAM10 affects additional developmental pathways required for cDC2 homeostasis.

There was also a significant overlap of differentially expressed genes (60%, 127 out of 212 genes), including *Cd207* (Langerin), between ADAM10-deficient cDC1, Notch2-deficient cDC1, and splenic CD103$^+$ DC (11) (Fig. 5*J* and Dataset S5*C*), suggesting that ADAM10-mediated Notch2 signaling is essential for the development and/or homeostasis of the splenic Langerin$^+$ cDC1 subset. Among the Notch2-related genes that were differentially expressed between ADAM10-deficient and control cDC1, 60 were also differentially expressed in ADAM10-deficient cDC2, indicating that the ADAM10–Notch2 axis regulates several developmental pathways shared by both cDC1 and cDC2.

ADAM10 Orchestrates EBI2-Mediated Migration and Positioning of cDC2 in the MZ. So far, we established that ADAM10-deficient ESAM^{hi} cDC2A (and their immediate precursors) exhibit a slower turnover and decreased survival. Appropriate positioning of CD4$^+$ cDC2 in the splenic MZ, controlled by the G protein–coupled receptor EBI2 (45, 46), is essential for their terminal differentiation and sentinel function (70). Together, this suggests that ADAM10 might control the maintenance of committed ESAM^{hi} cDC2A by regulating their migration into the appropriate MZ microanatomical niche. *Gpr183* mRNA (encoding for EBI2) is predominantly, but not exclusively, expressed by cDC2 and was significantly down-regulated in both ADAM10-deficient cDC1 and cDC2A subsets as compared to control cDC (Fig. 6*A*). Control SIRP-α$^+$ cDC2 migrated dose-dependently toward the EBI2 ligand 7α,25-Dihydroxycholesterol (7α,25-OHC) in an in vitro transwell migration assay, until receptor internalization abrogated cDC2 migration at high ligand concentrations, while ADAM10-deficient cDC2 completely failed to migrate in an EBI2-dependent manner (Fig. 6*B*). As reported before, mice deficient for EBI2 had fewer splenic SIRP-α$^+$ cDC2 (45, 46), but in contrast to ADAM10$^{\Delta CD11c}$ mice, the spleens of EBI2-KO mice were not completely depleted of ESAM^{hi} cDC2 (Fig. 6*C*). Since both ESAM^{hi} and CX$_3$CR1$^+$ cDC2 were reduced in EBI2-KO spleens (Fig. 6*D*), this indicates that additional pathways contribute to the regulation of ESAM^{hi} cDC2 homeostasis in ADAM10$^{\Delta CD11c}$ mice. Next to EBI2, cDC2 positioning in the splenic bridging channels is regulated by Sphingosine-1 Phosphate Receptor 1 (S1PR1) signaling (71). Although *S1pr1* expression was strongly up-regulated on cDC2A isolated from ADAM10$^{\Delta CD11c}$ mice (Fig. 6*E*), ADAM10-deficient cDC2 failed to migrate toward increasing concentrations of the S1PR1 ligand S1P in an in vitro transwell setting (Fig. 6*F*). Notably, neither control nor ADAM10-deficient CD8-α$^+$ cDC1 responded to chemoattract signals from 7α,25-OHC (Fig. 6*B*) or S1P (Fig. 6*F*). In line with this, EBI2-KO mice exhibited no differences in the number of splenic Langerin$^+$ cDC1 (Fig. 6*D*), indicating that proper MZ localization might not be crucial for terminal differentiation of ADAM10-deficient cDC1.

To determine whether ADAM10 intrinsically regulates ESAM^{hi} cDC2A migration, or whether the observed migration defects were due to abrogated EBI2 and S1PR1 responsiveness of the emerging ESAM^{lo} cDC2B population in ADAM10$^{\Delta CD11c}$ mice, we assessed WT cDC2 migration in the presence of the selective ADAM10 inhibitor GI254023X (72). Pharmacological ADAM10 inhibition significantly blocked WT cDC2 migration toward both 7α,25-OHC in a dose-dependent manner (Fig. 6*G*). Although ADAM10-inhibition abrogated EBI2-mediated migration

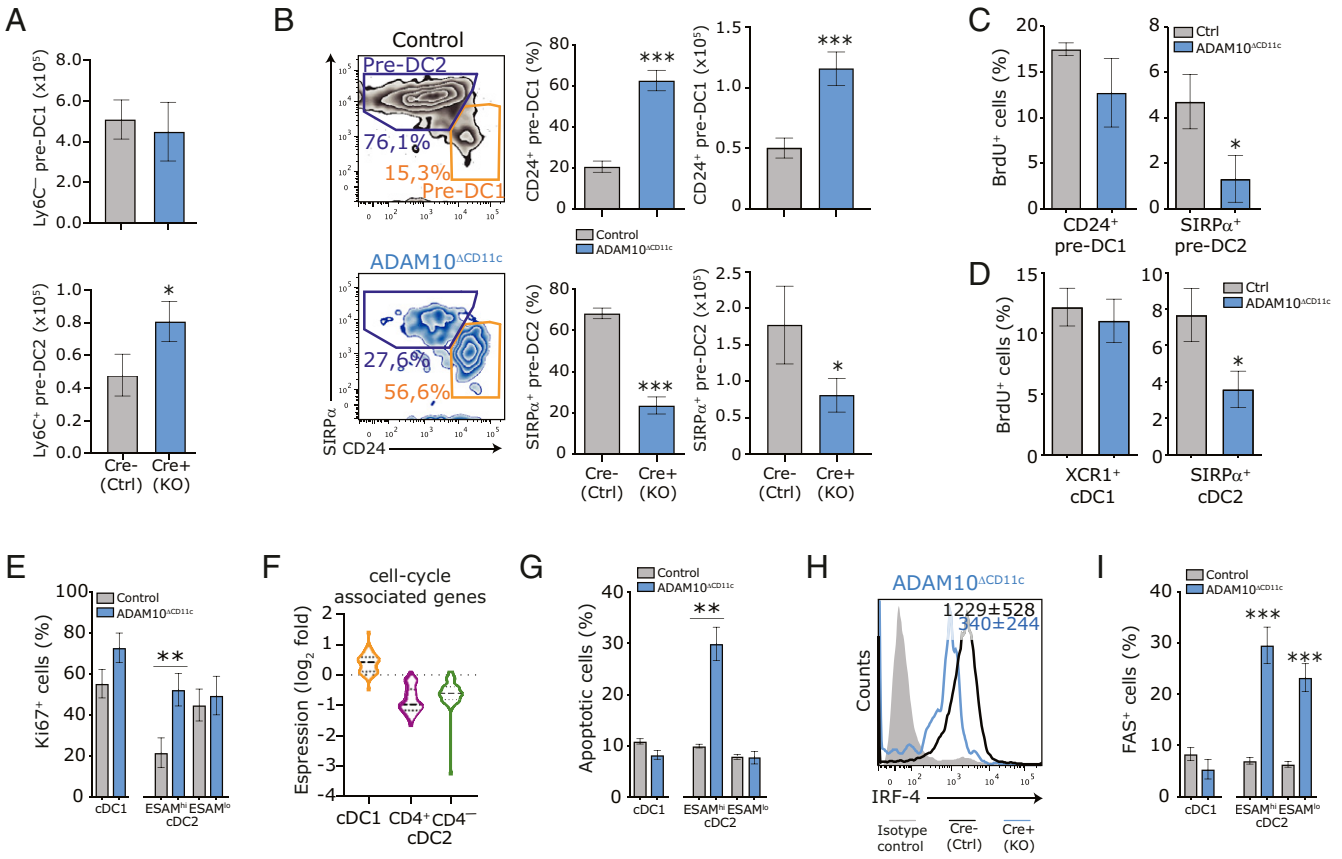

Fig. 4. ADAM10 is required for splenic cDC2 commitment and differentiation by impacting proliferation and cell survival. (*A*) Absolute numbers of committed Ly6C$^-$ preDC1 (*Top*) and Ly6C$^+$ preDC2 (*Bottom*) subsets in spleens of control and ADAM10$^{\Delta CD11c}$ mice. PrecDC were defined as Lin$^-$CD11c$^+$MHCII$^-$FLT3$^+$cells. (*B*) Flow cytometric analysis of SIRP-α and CD24 expression on CD11c$^+$MHCII$^+$CD11b$^-$CD8-α$^-$ cells, which represent natural immature stages of cDC2 (aubergine gate) and cDC1 (orange gate) development, respectively. Cells were isolated from control (*Top*) or ADAM10$^{\Delta CD11c}$ (*Bottom*) spleens. Bar graphs indicate the frequency and absolute numbers of these cells found in the spleen. Control or ADAM10$^{\Delta CD11c}$ mice were injected with BrdU and proliferating cells were detected 12 h later as BrdU$^+$ cells among splenic CD24$^+$ preDC1 and SIRP-α$^+$ preDC2 (*C*) or CD11c$^+$MHCII$^+$ mature splenic XCR1$^+$ cDC1 and SIRP-α$^+$ cDC2 (*D*). (*E*) Flow cytometry analysis for the expression of the proliferation-associated marker KI-67 in CD8-α$^+$ cDC1 and CD4$^+$ or CD4$^-$ cDC2 subsets isolated from control and ADAM10-deficient mice. (*F*) Violin plots showing expression of cell-cycle signature genes across bulk-sorted CD11c$^+$MHCII$^+$ CD8$^+$ cDC1 (orange), CD4$^+$ (purple), and CD4$^-$ (green) cDC2 subsets. Expression is $\log_2$ fold change between ADAM10 deficient/control. Gene sets are retrieved from the publication by Tirosh et al. (60). (*G*) The frequency of (7AAD$^+$Annexin V$^+$) apoptotic cells among splenic ESAM^{hi} and ESAM^{lo} cDC2 in control and ADAM10$^{\Delta CD11c}$ mice. (*H*) Flow cytometric analysis of IRF-4 expression in splenic CD11c$^+$MHCII$^+$ SIRP-α$^+$ cDC2. Cells were isolated from control or ADAM10$^{\Delta CD11c}$ mice. Filled histogram: isotype control. (*I*) The frequency of FAS (CD95)$^+$ cells among splenic cDC1 and cDC2 subsets in control and ADAM10$^{\Delta CD11c}$ mice. *$P <$ 0.05, **$P < 0.01$, and ***$P < 0.001$ (Student's *t* test); data are pooled from three or more experiments ($n = 3$ to 5 mice/experiment); FACS plots show one representative mouse/group with mean fluorescent intensity ± SEM.

of both WT ESAM^{hi} cDC2A and WT ESAM^{lo} cDC2B, the latter were less sensitive to GI254023X (Fig. 6*H*). In conclusion, these data demonstrate that ADAM10 directly governs EBI2- and S1PR1-dependent homing of cDC2, via yet unknown mechanisms, which is essential for appropriate positioning and the development of splenic cDC2A.

Discussion

To date, cDC subset development is mainly defined by differential TF dependencies, which indeed drive the major cDC1 and cDC2 lineage fate decisions (7, 23–26), but might fail to elucidate final cDC subset specifications that require tissue-specific cues (2). Indeed, as a fraction of mature splenic cDC is proliferating at any given time (54, 58, 71, 73), this indicates that cDC do not represent terminally differentiated cells inert to fine-tuning by external signals in situ but that the local microenvironment may contribute to the differentiation of the phenotypically and functionally distinct cDC subsets (74, 75). In agreement with two recent publications (35, 42), we demonstrate the requirement of ADAM10-mediated posttranslational protein modifications for appropriate differentiation of splenic ESAM^{hi} cDC2A. Beyond this observation, we establish that ADAM10 critically regulates cDC2 homeostasis via a complex interplay of signaling pathways involved in cell proliferation, survival, and energy metabolism. Moreover, we discovered the emergence of a splenic Clec12a$^+$CX$_3$CR1$^+$ESAM^{lo} cDC2B population in ADAM10$^{\Delta CD11c}$ mice so that the size of the cDC2 compartment as a whole remains comparable to control mice. Finally, we uncover that the ADAM10 requirement exceeds the cDC2 compartment, as ADAM10 is also essential for Langerin$^+$ cDC1 and MMM homeostasis. Hence, our data highlight that ADAM10-mediated ectodomain shedding on splenic CD11c$^+$ cells represents a crucial and nonredundant mechanism in shaping the MZ microenvironmental niche by fine-tuning the homeostasis of its major myeloid immune cell populations.

Recently, it was demonstrated that cell-autonomous shedding of FLT3L by ADAM10 is essential for the homeostasis of splenic ESAM^{hi} cDC2 (35). This study demonstrated an almost complete absence of splenic cDC2 in ADAM10$^{\Delta CD11c}$ mice, which is in strong contrast to our observations. Since the treatment with

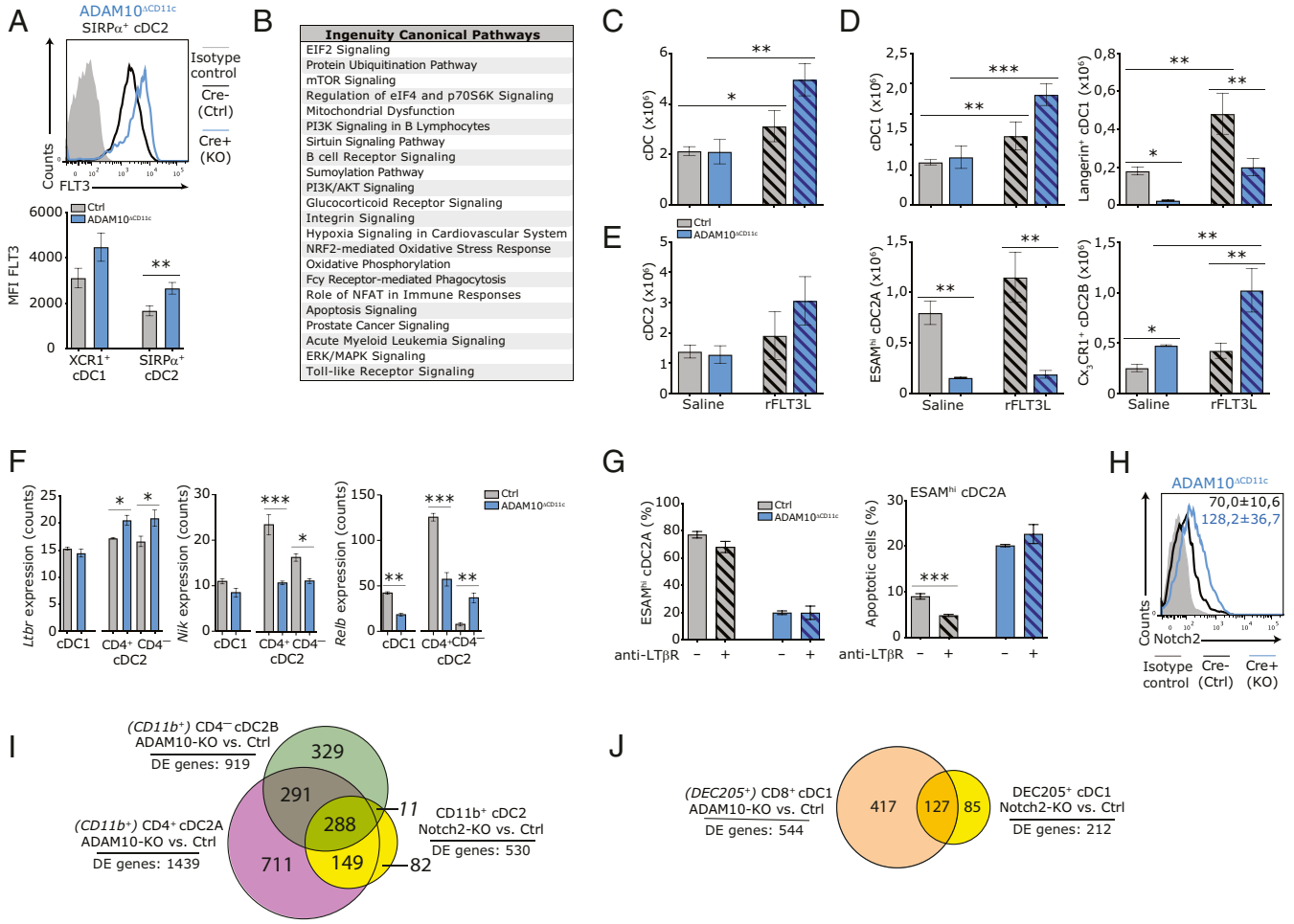

Fig. 5. ADAM10 controls splenic cDC2 homeostasis via Notch2-dependent but FLT3- and LT-βR–independent pathways. (*A*) FACS plot shows expression of cell-surface FLT3 on splenic SIRP-α$^+$ cDC2 from control (black) and ADAM10$^{\Delta CD11c}$ (blue) mice. Filled gray histogram: isotype control. Bar graph represents quantification of FLT3 expression (mean fluorescent intensities, MFI) on splenic XCR1$^+$ cDC1 and SIRP-α$^+$ cDC2 from control and ADAM10$^{\Delta CD11c}$ mice. (*B*) Canonical pathway analysis (Ingenuity) associated with significantly changed genes between bulk-sorted ADAM10-deficient/control CD4$^+$ cDC2A. Control and ADAM10$^{\Delta CD11c}$ mice were treated with recombinant FLT3 ligand (rFLT3L) or saline as control. (*C*) Absolute number of splenic cDC in saline and rFLT3L treated control and ADAM10$^{\Delta CD11c}$ mice. (*D*) Absolute number of splenic cDC1 (*Left*) and Langerin$^+$ cDC1 (*Right*) in saline and rFLT3L-treated control and ADAM10$^{\Delta CD11c}$ mice. (*E*) Absolute number of splenic cDC2 (*Left*), ESAM^{hi} cDC2A (*Middle*), and CX$_3$CR1$^+$ cDC2B (*Right*) in saline and rFLT3L-treated control and ADAM10$^{\Delta CD11c}$ mice. (*F*) *Ltbr*, *Nik*, and *Relb* mRNA expression in bulk-sorted control or ADAM10-deficient splenic CD8-α$^+$ cDC1, CD4$^+$ cDC2, and CD4$^-$ cDC2 subsets. (*G*) Control and ADAM10$^{\Delta CD11c}$ mice were treated with agonistic anti–LT-βR antibody or saline as control. Bar graphs shows the frequency of ESAM^{hi} cells among SIRP-α$^+$ cDC2 (*Left*) or the frequency of apoptotic cells within this population (*Right*) in saline-treated and antibody-treated control versus ADAM10$^{\Delta CD11c}$ mice. (*H*) Flow cytometric analysis of Notch2 expression on splenic CD11c$^+$MHCII$^+$SIRP-α$^+$ cDC2 from control (black line) and ADAM10$^{\Delta CD11c}$ (blue line) mice. Filled gray histogram: isotype control. (*I*) Venn diagram summarizing the pair-wise overlap of significant differentially expressed genes (DE genes) between ADAM10-deficient/control CD11c$^+$MHCII$^+$CD4$^+$ cDC2A (purple), ADAM10-deficient/control CD4$^-$ cDC2B (green), and Notch2-KO/control CD11b$^+$ cDC2 (yellow). Data from Notch2-KO/control CD11b$^+$ cDC2 are retrieved from GEO, accession no. GSE45698 (44). (*J*) Venn diagram summarizing the pair-wise overlap of significantly changed genes between ADAM10-deficient/control CD8-α$^+$ cDC2 (orange) and Notch2-KO/control CD205$^+$ cDC1 (yellow). Data from Notch2-KO/control CD205$^+$ cDC1 are retrieved from GEO, accession no. GSE45698 (44). *$P < 0.05$, **$P < 0.01$, and ***$P < 0.001$ (Student's *t* test); data are pooled from two or more experiments (n = 3 to 6 mice/experiment); FACS plots show one representative mouse/group with mean frequencies or mean fluorescent intensity ± SEM.

rFLT3L resulted in rescued splenic cDC2 in ADAM10$^{\Delta CD11c}$ mice to numbers that were comparable to WT mice, and because rFLT3L did not affect ESAM^{lo} cDC2 numbers, the authors argued that the cDC2 recovery in these mice was due to the expansion of ESAM^{hi} cDC2. In line with this, we demonstrate that ADAM10-deficient cDC2 exhibit significant differences in cell survival pathways like mTOR, PI3K/Akt, and Erk/Stat5 signaling that are downstream of FLT3. This suggests that the observed enhanced apoptosis of ADAM10-deficient cDC2 could be, at least partially, due to lack of FLT3 signaling. However, although our data also demonstrate an increase of cDC2 in ADAM10$^{\Delta CD11c}$ mice upon rFLT3L supplementation, this expansion was completely accounted for by the expansion of CX$_3$CR1$^+$ cDC2, and ESAM^{hi} cDC2 numbers could not be rescued. Therefore, our data demonstrate that FLT3 signaling is not crucial for the maintenance of ADAM10-deficient cDC2. Notably, we also observed that ADAM10-deficient Langerin$^+$ cDC1 actually expanded more strongly than control cells. However, this expansion of the small remaining Langerin$^+$ cDC1 population was not able to restore the numbers as found in control mice, indicating that FLT3 signaling does not contribute to the development and maintenance of splenic Langerin$^+$ cDC1 in ADAM10$^{\Delta CD11c}$ mice.

The role of ADAM10 in Notch signaling is well established. Indeed, ADAM10 deficiency results in the almost complete absence of the Notch2-dependent ESAM^{hi} splenic cDC2A subset (17, 38, 44). Furthermore, ADAM10-deficient cDC lack the

expression of Notch2-dependent genes and exhibit a significant overlap in gene expression with Notch2-KO cDC (44). However, Notch2 deficiency leads to reduced total splenic cDC2 counts (17, 38, 44), while ADAM10 deficiency prompts the emergence of a discrete cDC2B subset completely compensating for the loss of ADAM10-dependent cDC2A. Besides, we already observe defective SIRP-α^+ pre-DC2 development in the absence of ADAM10, which is corroborating the observation that Notch2 is not yet required at this developmental stage (17). In addition, a larger fraction of differentially regulated genes in ADAM10-deficient cDC2 and cDC1 are Notch2 independent. In accordance, overexpression of the active Notch intracellular signaling domain in ADAM10-deficient cDC2 is not able to rescue the ESAM^{hi} cDC2A subset (35). Therefore, we propose here that insufficient Notch2 signaling in ADAM10-deficient cDC is merely one mechanism by which ADAM10 regulates splenic cDC homeostasis and that ADAM10 regulates cDC development and homeostasis also via Notch2-independent mechanisms. For example, mice deficient in LT-α1β2, LT-βR, or RelB, a component of the downstream noncanonical NF-κB signaling pathway, exhibit reduced numbers of splenic ESAM^{hi} cDC2A especially due to their requirement for the homeostatic proliferation of these cells (17, 24, 58, 76, 77). Since ADAM10-deficient cDC2 reveal reduced expression of the NF-κB signaling components NIK and RelB, and because the phenotype of ADAM10$^{\Delta CD11c}$ mice overlaps with that of RelB-KO mice (78), ADAM10 deficiency may result in insufficient LT-βR signaling in cDC2. Nevertheless, cDC2 homeostasis in ADAM10$^{\Delta CD11c}$ mice cannot be rescued by treatment with agonistic anti–LT-βR antibodies, indicating that defective LT-βR signaling in ADAM10-deficient cDC2 does not contribute to the observed splenic cDC phenotype.

Within the spleen, EBI2- and S1PR1-mediated migration into the MZ provides ESAM^{hi} cDC2A access to critical growth factors, such as Notch2 and LT-βR signaling, emphasizing the importance of the MZ microanatomical niche for cDC2 homeostasis. Mechanistical insights in how ADAM10 might control EBI2 expression and cDC2 migration are still missing. Our data indicate that EBI2 is not a direct Notch2 or IRF4 target. EBI2-KO mice phenocopy the loss of SIRP-α^+ESAM^{hi} cDC2A seen in ADAM10$^{\Delta CD11c}$ mice, although EBI2 deficiency does not affect cDC2 apoptosis, and the remaining cDC2 retain expression of ESAM (45, 46). Therefore, our data suggest that even though ADAM10 might directly affect EBI2-mediated migration in vitro, the control of cDC2 homeostasis and differentiation by ADAM10 in situ is regulated at multiple levels during cDC development and differentiation. For example, ADAM10 deficiency also affects S1P-dependent cDC2 migration, suggesting that ADAM10 might regulate general migration pathways in cDC.

Notably, in the absence of ADAM10, the physiologic number of total splenic cDC2 is maintained by the emergence of a Clec12a$^+$CX$_3$CR1$^+$ESAM^{lo} cDC2B population. The exact developmental origin of this emerging cDC2B subset is unknown, but these cells are distinct from the cDC2B subset present in the steady-state spleen. ESAM^{lo} cDC2B in ADAM10$^{\Delta CD11c}$ might

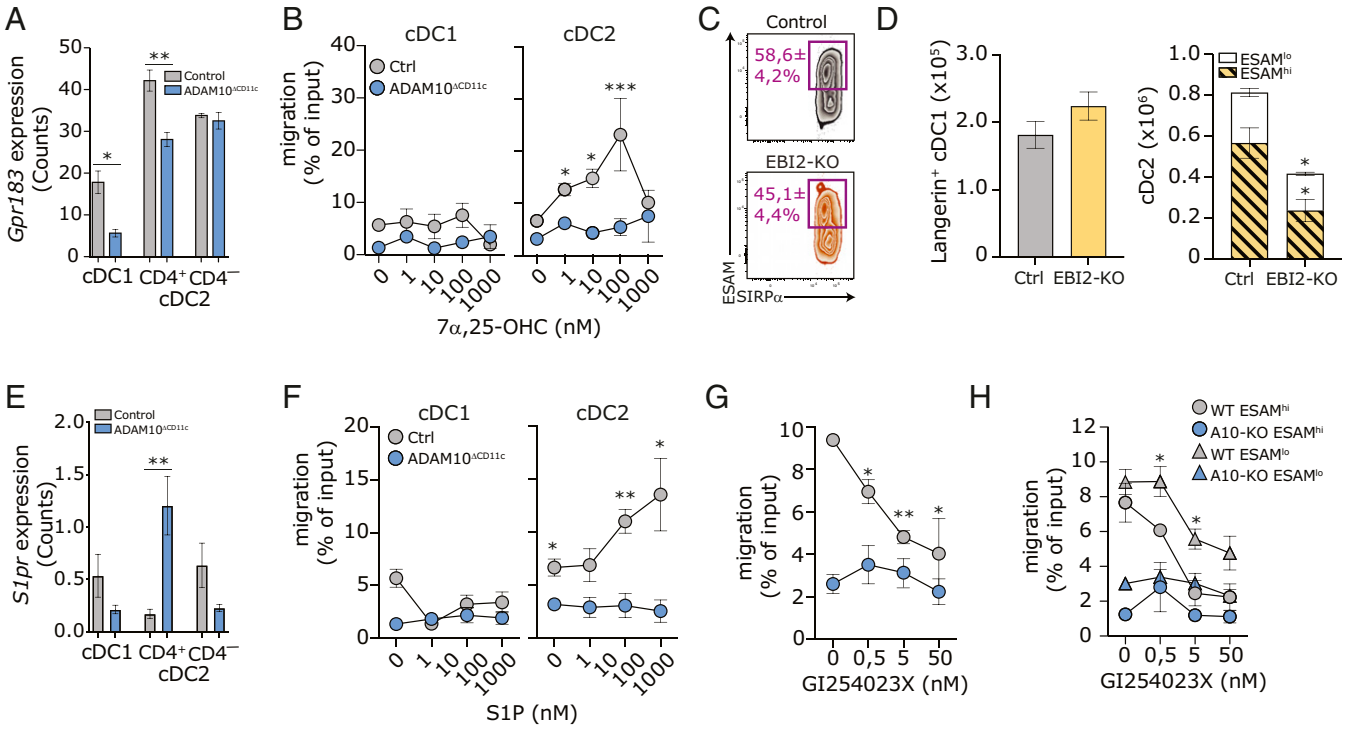

Fig. 6. ADAM10 regulates EBI2-mediated migration of cDC2 in vitro. (*A*) *Gpr183* (Ebi2) transcript expression in bulk-sorted control or ADAM10-deficient splenic CD8-α^+ cDC1, CD4$^+$ cDC2, and CD4$^-$ cDC2. (*B*) In vitro transwell migration of CD11c-purified control and ADAM10-deficient cDC toward indicated concentrations of 7α,25-OHC. Migration was calculated as the ratio of the number of cells migrating with/without chemoattractant; migration of cDC1 and cDC2 subsets was determined by staining for XCR1 and SIRP-α, respectively. (*C*) Representative flow cytometry plot with average frequencies of splenic ESAM^{hi}SIRP-α^+ cDC2 in control and ADAM10$^{\Delta CD11c}$ mice. (*D*) Absolute numbers of splenic Langerin$^+$ cDC1 (*Left*) and absolute cell counts of splenic ESAM^{hi} and ESAM^{lo} SIRP-α^+ cDC2 (*Right*) in control and EBI2-KO mice. (*E*) *S1pr* transcript expression in bulk-sorted control or ADAM10-deficient splenic CD8-α^+ cDC1, CD4$^+$ cDC2, and CD4$^-$ cDC2. (*F*) In vitro transwell migration of CD11c-purified control and ADAM10-deficient cDC toward indicated concentrations of S1P. (*G*) In vitro transwell migration of WT and ADAM10-deficient CD11c-purified cDC toward 10 μM 7α,25-OHC in the presence of indicated concentrations of the ADAM10-inhibitor GI254023X. (*H*) In vitro transwell migration of ESAM^{hi} and ESAM^{lo} cDC2 in the presences of ADAM10-inhibition as in *F*. *P < 0.05, **P < 0.01, and ***P < 0.001 (Student's t test). Migration data represent mean frequencies ± SEM of four pooled experiments (n = 3 mice/experiment), while bulk RNA-seq and SC-seq-WTA data both represent three control and three ADAM10-deficient samples.

comprise Mo-DC, as they preferentially express monocyte-specific genes (35), although much lower than monocytes or macrophages. However, our data indicate that the emerging ESAM^{lo} cDC2B are rather bona fide cDC2B expressing the cDC-specific TF PU.1 and ZBTB46. Moreover, ADAM10-deficient cDC2B strongly expand upon rFLT3L treatment. ESAM^{lo} cDC2B do not seem to derive from monocytes nor CDP (17, 79), and it is suggested that both cDC2A and cDC2B arise from pre-DC of which the commitment into either cDC2A or cDC2B is instructed by the local tissue microenvironment (16). Why then ADAM10 specifically impacts cDC2A and not cDC2B differentiation, especially in the light of the reduced commitment and proliferation of pre-DC2, is still unclear. However, both cDC2A and cDC2B can originate from ROR-γt^{+} precursors (16), suggesting that the default differentiation step of precDC2 is toward cDC2B and that additional ADAM10-mediated differentiation cues (e.g., localization within the MZ and Notch2 signaling) are required for the generation of mature ESAM^{hi} cDC2A. Our data indicate that splenic ADAM10-deficient ESAM^{lo} cDC2B most likely represent a diverging branch of lymphoid-tissue cDC2B that share a prominent gene expression signature with pLN-resident cDC2. This emphasizes the heterogeneity within the cDC2B compartment and reveals a role of ADAM10 in controlling the bifurcation and lineage identity of cDC2A and cDC2B. The existence of different cDC2B subsets may explain why ADAM10 deficiency does not affect pLN cDC2 homeostasis and suggests that cDC2B subsets follow distinct developmental pathways or depend on different programming by the local microenvironment.

Beyond cDC2, our observations highlight the critical role of ADAM10 within the cDC1 compartment, where its absence abrogates the development of Langerin^{+} cDC1. Recent studies have shown that among cDC1, in particular, this Langerin^{+} cDC1 subset contributes to key cDC1 functions like cross-presentation and CD4^{+} Th1 cell induction (1, 11–14). So far, conclusive evidence about the ontogeny and subset relationship of Langerin^{+} cDC1 is lacking. Langerin-expression on cDC1 may represent distinct developmental stages within the splenic cDC1 population, where Langerin^{-} cDC1 constitute the precursors of the functionally more mature Langerin^{+} state (1). While ADAM10 is essential for early cDC2 development, it is dispensable for cDC1 commitment as ADAM10 appears to support the terminal differentiation into Langerin^{+} cDC1 cells. Since Langerin^{+} and Langerin^{-} cDC1 share their dependence on certain TF, including IRF8 and Batf3, both subsets presumably differentiate from the same precursors (1, 13). Thus, our data suggest a selective requirement of ADAM10 for the terminal differentiation of splenic cDC1 into Langerin^{+} cDC1, which depends on Notch2 signaling and other developmental factors. Mature XCR1^{+} cDC1 do not express CX_3CR1; however, both ADAM10$^{\Delta XCR1}$ and ADAM10$^{\Delta CX3CR1}$ mice exhibit a drastic reduction in the number of splenic Langerin^{+} cDC1. Although this might suggest additional extrinsic control of Langerin^{+} cDC1 homeostasis, pre-DC are CX_3CR1 positive, and therefore the effects seen in ADAM10$^{\Delta CX3CR1}$ mice are likely due to Cre-mediated ADAM10 deletion at early stages of cDC1 development (80).

The pivotal role of macrophages in tissue homeostasis, in particular at the interface of the MZ, is reflected by the phenotypic and functional heterogeneity of CD11c^{+} macrophage populations (3). Although the factors regulating MMM development and maintenance in the spleen are largely unknown, here we demonstrate that both *CD11c*-Cre and *CX_3CR1*-Cre–mediated deletion of ADAM10 increase the number of MMM and that these MMM are affected in their localization in situ. Although, the changes within the splenic cDC compartment might indirectly impair MMM homeostasis via a lack of chemokines and/or growth factors provided by the missing cDC, our data so far exclude any role of XCR1^{+} cDC1 in regulating MMM homeostasis. Therefore, we rather argue for a cell-intrinsic negative regulatory role of ADAM10 shedding on MMM homeostasis.

ADAM10 and ADAM17 are involved in the shedding of more than 70 known substrates (31, 32, 34, 81–86). Whereas certain substrates are specifically shed by either ADAM10 or ADAM17, many of these substrates can be processed by both ADAMs. Although ADAM10 and ADAM17 are similar in sequence and structure, we prove that ADAM10, but not ADAM17, is essential for splenic cDC1 and cDC2 homeostasis. This underlines that ADAM10 and ADAM17 activity in vivo is spatially and/or temporally regulated within a particular cell or tissue, ensuring functional specialization of the two proteases. For example, proteolytic cleavage of CX_3CL1 under steady-state conditions is mediated by ADAM10, while during inflammation shedding is executed by ADAM17 (87, 88). Notably, our analysis reveals that ADAM10/17$^{\Delta CD11c}$ DKO mice faithfully phenocopy ADAM10$^{\Delta CD11c}$ single KO, excluding any compensatory effects of ADAM17 and emphasizing that the spatial and/or temporal regulation of the two sheddases in the spleen is reliably maintained in the absence of ADAM10.

In summary, we identified several pathways by which ADAM10 governs critical aspects of cDC biology. ADAM10 is not only essential for the development and survival of pre-cDC2, and for cDC2 localization and final differentiation within the unique microenvironment of the MZ, but it also regulates the terminal differentiation of cDC1 and the homeostasis of MMM. Thus, our data highlight the significance of posttranslational modifications for shaping the unique and dynamic microenvironment of the MZ and reveal an unexpected complexity of CD11c-specific ADAM10 shedding on the homeostasis of a broad range of splenic myeloid cells.

Data Availability. RNA sequencing data have been deposited in GEO (GSE154309 and GSE154767). All other study data are included in the article and/or supporting information.

ACKNOWLEDGMENTS. We thank A. Brand, C. Hessel, T. Klaus, S. Papaioannou, and all other members of the B.E.C. laboratory for support and advice; A. Nikolaev for help with microscopy; and M. Backer, J. M. M. den Haan, J. D. Laman, and A. Waisman for suggestions and critical reading of the manuscript. FACS sorting and RNA sequencing were supported by core facilities of the Research Center for Immunotherapy, University Medical Center Mainz. This work was supported by grants from the German Research Foundation to R.A.B. (BA 5939/2-1) and B.E.C. (CL 419/2-1 and CL 419/4-1).

1. R. A. Backer, N. Diener, B. E. Clausen, Langerin^{+}CD8^{+} dendritic cells in the splenic marginal zone: Not so marginal after all. *Front. Immunol.* **10**, 741 (2019).
2. S. C. Eisenbarth, Dendritic cell subsets in T cell programming: Location dictates function. *Nat. Rev. Immunol.* **19**, 89–103 (2019).
3. J. M. den Haan, G. Kraal, Innate immune functions of macrophage subpopulations in the spleen. *J. Innate Immun.* **4**, 437–445 (2012).
4. M. Guilliams *et al*., Dendritic cells, monocytes and macrophages: A unified nomenclature based on ontogeny. *Nat. Rev. Immunol.* **14**, 571–578 (2014).
5. M. Merad, P. Sathe, J. Helft, J. Miller, A. Mortha, The dendritic cell lineage: Ontogeny and function of dendritic cells and their subsets in the steady state and the inflamed setting. *Annu. Rev. Immunol.* **31**, 563–604 (2013).
6. B. U. Schraml, C. Reis e Sousa, Defining dendritic cells. *Curr. Opin. Immunol.* **32**, 13–20 (2015).
7. A. Mildner, S. Jung, Development and function of dendritic cell subsets. *Immunity* **40**, 642–656 (2014).
8. V. Durai, K. M. Murphy, Functions of murine dendritic cells. *Immunity* **45**, 719–736 (2016).
9. C. Macri, E. S. Pang, T. Patton, M. O'Keeffe, Dendritic cell subsets. *Semin. Cell Dev. Biol.* **84**, 11–21 (2018).
10. J. Idoyaga, N. Suda, K. Suda, C. G. Park, R. M. Steinman, Antibody to Langerin/CD207 localizes large numbers of CD8alpha+ dendritic cells to the marginal zone of mouse spleen. *Proc. Natl. Acad. Sci. U.S.A.* **106**, 1524–1529 (2009).
11. C. H. Qiu *et al*., Novel subset of CD8alpha+ dendritic cells localized in the marginal zone is responsible for tolerance to cell-associated antigens. *J. Immunol.* **182**, 4127–4136 (2009).
12. K. J. Farrand *et al*., Langerin+ CD8alpha+ dendritic cells are critical for cross-priming and IL-12 production in response to systemic antigens. *J. Immunol.* **183**, 7732–7742 (2009).
13. T. R. Petersen, D. A. Knight, C. W. Tang, T. L. Osmond, I. F. Hermans, Batf3-independent langerin- CX3CR1- CD8α+ splenic DCs represent a precursor for classical cross-presenting CD8α+ DCs. *J. Leukoc. Biol.* **96**, 1001–1010 (2014).

14. K. A. Prendergast, N. J. Daniels, T. R. Petersen, I. F. Hermans, J. R. Kirman, Langerin^{+} CD8α^{+} dendritic cells drive early CD8^{+} T cell activation and IL-12 production during systemic bacterial infection. *Front. Immunol.* **9**, 953 (2018).
15. M. Guilliams *et al*., Unsupervised high-dimensional analysis aligns dendritic cells across tissues and species. *Immunity* **45**, 669–684 (2016).
16. C. C. Brown *et al*., Transcriptional basis of mouse and human dendritic cell heterogeneity. *Cell* **179**, 846–863.e24 (2019).
17. K. L. Lewis *et al*., Notch2 receptor signaling controls functional differentiation of dendritic cells in the spleen and intestine. *Immunity* **35**, 780–791 (2011).
18. S. Kasahara, E. A. Clark, Dendritic cell-associated lectin 2 (DCAL2) defines a distinct CD8α-dendritic cell subset. *J. Leukoc. Biol.* **91**, 437–448 (2012).
19. Y. Kumamoto *et al*., CD301b^{+} dermal dendritic cells drive T helper 2 cell-mediated immunity. *Immunity* **39**, 733–743 (2013).
20. Y. Gao *et al*., Control of T helper 2 responses by transcription factor IRF4-dependent dendritic cells. *Immunity* **39**, 722–732 (2013).
21. S. W. Kashem *et al*., Nociceptive sensory fibers drive Interleukin-23 production from CD301b+ dermal dendritic cells and drive protective cutaneous immunity. *Immunity* **43**, 515–526 (2015).
22. J. L. Linehan *et al*., Generation of Th17 cells in response to intranasal infection requires TGF-β1 from dendritic cells and IL-6 from CD301b+ dendritic cells. *Proc. Natl. Acad. Sci. U.S.A.* **112**, 12782–12787 (2015).
23. G. T. Belz, S. L. Nutt, Transcriptional programming of the dendritic cell network. *Nat. Rev. Immunol.* **12**, 101–113 (2012).
24. T. L. Murphy *et al*., Transcriptional control of dendritic cell development. *Annu. Rev. Immunol.* **34**, 93–119 (2016).
25. L. Amon *et al*., Transcriptional control of dendritic cell development and functions. *Int. Rev. Cell Mol. Biol.* **349**, 55–151 (2019).
26. R. Tussiwand, E. L. Gautier, Transcriptional regulation of mononuclear phagocyte development. *Front. Immunol.* **6**, 533 (2015).
27. D. Sichien, B. N. Lambrecht, M. Guilliams, C. L. Scott, Development of conventional dendritic cells: From common bone marrow progenitors to multiple subsets in peripheral tissues. *Mucosal Immunol.* **10**, 831–844 (2017).
28. G. Murphy, The ADAMs: Signalling scissors in the tumour microenvironment. *Nat. Rev. Cancer* **8**, 929–941 (2008).
29. J. Müllberg, K. Althoff, T. Jostock, S. Rose-John, The importance of shedding of membrane proteins for cytokine biology. *Eur. Cytokine Netw.* **11**, 27–38 (2000).
30. S. Rose-John, J. Scheller, G. Elson, S. A. Jones, Interleukin-6 biology is coordinated by membrane-bound and soluble receptors: Role in inflammation and cancer. *J. Leukoc. Biol.* **80**, 227–236 (2006).
31. K. Reiss, P. Saftig, The "a disintegrin and metalloprotease" (ADAM) family of sheddases: Physiological and cellular functions. *Semin. Cell Dev. Biol.* **20**, 126–137 (2009).
32. J. Scheller, A. Chalaris, C. Garbers, S. Rose-John, ADAM17: A molecular switch to control inflammation and tissue regeneration. *Trends Immunol.* **32**, 380–387 (2011).
33. D. Dreymueller, S. Uhlig, A. Ludwig, ADAM-family metalloproteinases in lung inflammation: Potential therapeutic targets. *Am. J. Physiol. Lung Cell. Mol. Physiol.* **308**, L325–L343 (2015).
34. B. N. Lambrecht, M. Vanderkerken, H. Hammad, The emerging role of ADAM metalloproteinases in immunity. *Nat. Rev. Immunol.* **18**, 745–758 (2018).
35. K. Fujita *et al*., Cell-autonomous FLT3L shedding via ADAM10 mediates conventional dendritic cell development in mouse spleen. *Proc. Natl. Acad. Sci. U.S.A.* **116**, 14714–14723 (2019).
36. E. Jorissen *et al*., The disintegrin/metalloproteinase ADAM10 is essential for the establishment of the brain cortex. *J. Neurosci.* **30**, 4833–4844 (2010).
37. K. Horiuchi *et al*., Cutting edge: TNF-alpha-converting enzyme (TACE/ADAM17) inactivation in mouse myeloid cells prevents lethality from endotoxin shock. *J. Immunol.* **179**, 2686–2689 (2007).
38. M. L. Caton, M. R. Smith-Raska, B. Reizis, Notch-RBP-J signaling controls the homeostasis of CD8- dendritic cells in the spleen. *J. Exp. Med.* **204**, 1653–1664 (2007).
39. S. Yona *et al*., Fate mapping reveals origins and dynamics of monocytes and tissue macrophages under homeostasis. *Immunity* **38**, 79–91 (2013).
40. T. Ohta *et al*., Crucial roles of XCR1-expressing dendritic cells and the XCR1-XCL1 chemokine axis in intestinal immune homeostasis. *Sci. Rep.* **6**, 23505 (2016).
41. F. Wanke *et al*., EBI2 is highly expressed in multiple sclerosis lesions and promotes early CNS migration of encephalitogenic CD4 T cells. *Cell Rep.* **18**, 1270–1284 (2017).
42. M. Vanderkerken *et al*., TAO-kinase 3 governs the terminal differentiation of NOTCH2-dependent splenic conventional dendritic cells. *Proc. Natl. Acad. Sci. U.S.A.* **117**, 31331–31342 (2020).
43. L. Bar-On *et al*., CX3CR1+ CD8alpha+ dendritic cells are a steady-state population related to plasmacytoid dendritic cells. *Proc. Natl. Acad. Sci. U.S.A.* **107**, 14745–14750 (2010).
44. A. T. Satpathy *et al*., Notch2-dependent classical dendritic cells orchestrate intestinal immunity to attaching-and-effacing bacterial pathogens. *Nat. Immunol.* **14**, 937–948 (2013).
45. T. Yi, J. G. Cyster, EBI2-mediated bridging channel positioning supports splenic dendritic cell homeostasis and particulate antigen capture. *eLife* **2**, e00757 (2013).
46. D. Gatto *et al*., The chemotactic receptor EBI2 regulates the homeostasis, localization and immunological function of splenic dendritic cells. *Nat. Immunol.* **14**, 446–453 (2013).
47. D. Dudziak *et al*., Differential antigen processing by dendritic cell subsets in vivo. *Science* **315**, 107–111 (2007).
48. S. Calabro *et al*., Differential intrasplenic migration of dendritic cell subsets tailors adaptive immunity. *Cell Rep.* **16**, 2472–2485 (2016).
49. J. Dicken *et al*., Transcriptional reprogramming of CD11b+Esam(hi) dendritic cell identity and function by loss of Runx3. *PLoS One* **8**, e77490 (2013).
50. H. Karsunky, M. Merad, A. Cozzio, I. L. Weissman, M. G. Manz, Flt3 ligand regulates dendritic cell development from Flt3+ lymphoid and myeloid-committed progenitors to Flt3+ dendritic cells in vivo. *J. Exp. Med.* **198**, 305–313 (2003).
51. C. Langlet *et al*., CD64 expression distinguishes monocyte-derived and conventional dendritic cells and reveals their distinct role during intramuscular immunization. *J. Immunol.* **188**, 1751–1760 (2012).
52. C. Bosteels *et al*., Inflammatory Type 2 cDCs acquire features of cDC1s and macrophages to orchestrate immunity to respiratory virus infection. *Immunity* **52**, 1039–1056.e9 (2020).
53. K. G. Elpek *et al*., Lymphoid organ-resident dendritic cells exhibit unique transcriptional fingerprints based on subset and site. *PLoS One* **6**, e23921 (2011).
54. S. H. Naik *et al*., Intrasplenic steady-state dendritic cell precursors that are distinct from monocytes. *Nat. Immunol.* **7**, 663–671 (2006).
55. K. Liu *et al*., Origin of dendritic cells in peripheral lymphoid organs of mice. *Nat. Immunol.* **8**, 578–583 (2007).
56. G. E. Grajales-Reyes *et al*., Batf3 maintains autoactivation of Irf8 for commitment of a CD8α(+) conventional DC clonogenic progenitor. *Nat. Immunol.* **16**, 708–717 (2015).
57. A. Schlitzer *et al*., Identification of cDC1- and cDC2-committed DC progenitors reveals early lineage priming at the common DC progenitor stage in the bone marrow. *Nat. Immunol.* **16**, 718–728 (2015).
58. K. Kabashima *et al*., Intrinsic lymphotoxin-beta receptor requirement for homeostasis of lymphoid tissue dendritic cells. *Immunity* **22**, 439–450 (2005).
59. J. Diao *et al*., In situ replication of immediate dendritic cell (DC) precursors contributes to conventional DC homeostasis in lymphoid tissue. *J. Immunol.* **176**, 7196–7206 (2006).
60. I. Tirosh *et al*., Dissecting the multicellular ecosystem of metastatic melanoma by single-cell RNA-seq. *Science* **352**, 189–196 (2016).
61. T. Tamura *et al*., IFN regulatory factor-4 and -8 govern dendritic cell subset development and their functional diversity. *J. Immunol.* **174**, 2573–2581 (2005).
62. A. Schlitzer *et al*., IRF4 transcription factor-dependent CD11b+ dendritic cells in human and mouse control mucosal IL-17 cytokine responses. *Immunity* **38**, 970–983 (2013).
63. S. Bajaña, K. Roach, S. Turner, J. Paul, S. Kovats, IRF4 promotes cutaneous dendritic cell migration to lymph nodes during homeostasis and inflammation. *J. Immunol.* **189**, 3368–3377 (2012).
64. E. K. Persson *et al*., IRF4 transcription-factor-dependent CD103(+)CD11b(+) dendritic cells drive mucosal T helper 17 cell differentiation. *Immunity* **38**, 958–969 (2013).
65. J. W. Williams *et al*., Transcription factor IRF4 drives dendritic cells to promote Th2 differentiation. *Nat. Commun.* **4**, 2990 (2013).
66. C. De Trez *et al*., The inhibitory HVEM-BTLA pathway counter regulates lymphotoxin receptor signaling to achieve homeostasis of dendritic cells. *J. Immunol.* **180**, 238–248 (2008).
67. J. Young *et al*., Lymphotoxin-alphabeta heterotrimers are cleaved by metalloproteinases and contribute to synovitis in rheumatoid arthritis. *Cytokine* **51**, 78–86 (2010).
68. A. J. Groot, M. A. Vooijs, The role of Adams in notch signaling. *Adv. Exp. Med. Biol.* **727**, 15–36 (2012).
69. A. C. Stanley *et al*., Critical roles for LIGHT and its receptors in generating T cell-mediated immunity during *Leishmania donovani* infection. *PLoS Pathog.* **7**, e1002279 (2011).
70. N. Fasnacht *et al*., Specific fibroblastic niches in secondary lymphoid organs orchestrate distinct Notch-regulated immune responses. *J. Exp. Med.* **211**, 2265–2279 (2014).
71. N. Czeloth *et al*., Sphingosine-1 phosphate signaling regulates positioning of dendritic cells within the spleen. *J. Immunol.* **179**, 5855–5863 (2007).
72. A. Ludwig *et al*., Metalloproteinase inhibitors for the disintegrin-like metalloproteinases ADAM10 and ADAM17 that differentially block constitutive and phorbol ester-inducible shedding of cell surface molecules. *Comb. Chem. High Throughput Screen.* **8**, 161–171 (2005).
73. F. Ginhoux *et al*., The origin and development of nonlymphoid tissue CD103+ DCs. *J. Exp. Med.* **206**, 3115–3130 (2009).
74. K. Liu *et al*., In vivo analysis of dendritic cell development and homeostasis. *Science* **324**, 392–397 (2009).
75. C. A. Klebanoff *et al*., Retinoic acid controls the homeostasis of pre-cDC-derived splenic and intestinal dendritic cells. *J. Exp. Med.* **210**, 1961–1976 (2013).
76. Y. G. Wang, K. D. Kim, J. Wang, P. Yu, Y. X. Fu, Stimulating lymphotoxin beta receptor on the dendritic cells is critical for their homeostasis and expansion. *J. Immunol.* **175**, 6997–7002 (2005).
77. Q. Wu *et al*., The requirement of membrane lymphotoxin for the presence of dendritic cells in lymphoid tissues. *J. Exp. Med.* **190**, 629–638 (1999).
78. L. Wu *et al*., RelB is essential for the development of myeloid-related CD8alpha- dendritic cells but not of lymphoid-related CD8alpha+ dendritic cells. *Immunity* **9**, 839–847 (1998).
79. C. Varol *et al*., Monocytes give rise to mucosal, but not splenic, conventional dendritic cells. *J. Exp. Med.* **204**, 171–180 (2007).
80. S. J. Cook *et al*., Differential chemokine receptor expression and usage by pre-cDC1 and pre-cDC2. *Immunol. Cell Biol.* **96**, 1131–1139 (2018).
81. S. J. Levine, Molecular mechanisms of soluble cytokine receptor generation. *J. Biol. Chem.* **283**, 14177–14181 (2008).
82. P. Saftig, K. Reiss, The "A Disintegrin And Metalloproteases" ADAM10 and ADAM17: Novel drug targets with therapeutic potential? *Eur. J. Cell Biol.* **90**, 527–535 (2011).
83. S. Rose-John, A. Chalaris, ADAM17: A potential therapeutic target for rheumatoid arthritis? *Int. J. Clin. Rheumatol.* **7**, 357–359 (2012).
84. J. Pruessmeyer, A. Ludwig, The good, the bad and the ugly substrates for ADAM10 and ADAM17 in brain pathology, inflammation and cancer. *Semin. Cell Dev. Biol.* **20**, 164–174 (2009).
85. F. S. Hoffmann *et al*., The immunoregulator soluble TACI is released by ADAM10 and reflects B cell activation in autoimmunity. *J. Immunol.* **194**, 542–552 (2015).
86. I. Yan *et al*., ADAM17 controls IL-6 signaling by cleavage of the murine IL-6Ralpha from the cell surface of leukocytes during inflammatory responses. *J. Leukoc. Biol.* **99**, 749–760 (2016).
87. C. Hundhausen *et al*., The disintegrin-like metalloproteinase ADAM10 is involved in constitutive cleavage of CX3CL1 (fractalkine) and regulates CX3CL1-mediated cell-cell adhesion. *Blood* **102**, 1186–1195 (2003).
88. K. J. Garton *et al*., Tumor necrosis factor-alpha-converting enzyme (ADAM17) mediates the cleavage and shedding of fractalkine (CX3CL1). *J. Biol. Chem.* **276**, 37993–38001 (2001).